

Multi-Granularity Hand Action Detection

Ting Zhe
School of Computer Science
Wuhan University
Wuhan, China
zheting@whu.edu.cn

Jing Zhang
The University of Sydney
Sydney, Australia
jingzhang.cv@gmail.com

Yongqian Li
School of Computer Science
Wuhan University
Wuhan, China
yongqianli@whu.edu.cn

Yong Luo[†]
Wuhan University &
Hubei LuoJia Laboratory
Wuhan, China
luoyong@whu.edu.cn

Han Hu
Beijing Institute of Technology
Beijing, China
hhu@bit.edu.cn

Dacheng Tao
Nanyang Technological University
Singapore, Singapore
dacheng.tao@ntu.edu.sg

Abstract

Detecting hand actions in videos is crucial for understanding video content and has diverse real-world applications. Existing approaches often focus on whole-body actions or coarse-grained action categories, lacking fine-grained hand-action localization information. To fill this gap, we introduce the **FHA-Kitchens** (Fine-Grained Hand Actions in Kitchen Scenes) dataset, providing both coarse- and fine-grained hand action categories along with localization annotations. This dataset comprises 2,377 video clips and 30,047 frames, annotated with approximately 200k bounding boxes and 880 action categories. Evaluation of existing action detection methods on FHA-Kitchens reveals varying generalization capabilities across different granularities. To handle multi-granularity in hand actions, we propose **MG-HAD**, an End-to-End Multi-Granularity Hand Action Detection method. It incorporates two new designs: Multi-dimensional Action Queries and Coarse-Fine Contrastive Denoising. Extensive experiments demonstrate MG-HAD's effectiveness for multi-granularity hand action detection, highlighting the significance of FHA-Kitchens for future research and real-world applications. The dataset and source code are available at MG-HAD.

CCS Concepts

• Computing methodologies → Activity recognition and understanding.

Keywords

Hand Action Detection, Dataset, Multi-Granularity

ACM Reference Format:

Ting Zhe, Jing Zhang, Yongqian Li, Yong Luo[†], Han Hu, and Dacheng Tao. 2024. Multi-Granularity Hand Action Detection. In *Proceedings of the 32nd ACM International Conference on Multimedia (MM '24)*, October 28–November 1, 2024, Melbourne, VIC, Australia.

[†]Corresponding author: Yong Luo.

Permission to make digital or hard copies of all or part of this work for personal or classroom use is granted without fee provided that copies are not made or distributed for profit or commercial advantage and that copies bear this notice and the full citation on the first page. Copyrights for components of this work owned by others than the author(s) must be honored. Abstracting with credit is permitted. To copy otherwise, or republish, to post on servers or to redistribute to lists, requires prior specific permission and/or a fee. Request permissions from permissions@acm.org.

MM '24, October 28–November 1, 2024, Melbourne, VIC, Australia

© 2024 Copyright held by the owner/author(s). Publication rights licensed to ACM.

ACM ISBN 979-8-4007-0686-8/24/10

<https://doi.org/10.1145/3664647.3680723>



Figure 1: Overview of the FHA-Kitchens dataset. (a) The annotation of hand actions in existing relevant datasets, where UCF101 [1] and Kinetics700 [2] are whole-body action datasets, while MPII Cooking [3] and EPIC KITCHENS [4] are hand action datasets. (b) The annotation of hand actions in our dataset. The left shows some frames extracted from 8 dish categories. The right illustrates the annotation process of hand actions in “fry vegetable”.

1, 2024, Melbourne, VIC, Australia. ACM, New York, NY, USA, 30 pages.
<https://doi.org/10.1145/3664647.3680723>

1 Introduction

Action detection, a crucial task in video understanding, aims to locate and recognize action instances in each video frame, with applications in various fields [5] such as Human-Computer Interaction (HCI) [6], Smart Homes [7], the Design and Control of Robot Hands [8], and Healthcare [9]. Despite significant advancements in action recognition regarding both large-scale benchmarks [1, 10] and advanced algorithms [11–13], action detection remains relatively underexplored, mainly due to the lack of datasets with spatial action localization annotations. Moreover, existing methods predominantly focus on whole-body actions, overlooking the fine-grained actions of specific body parts, such as hands. However, hand

actions are integral to daily activities, underscoring the significant research and practical importance of hand action detection.

Pioneering datasets such as MPII Cooking Activities [3] and EPIC-KITCHENS [4] have been developed to facilitate hand-action research. However, they exhibit limitations including insufficient representation of hand-action granularity, lack of annotation of hand-action interaction regions, and neglect of the relationships between interacting objects. As shown in Figure 1(a), they offer only coarse-grained annotations for hand actions like “*cut*” rather than the fine-grained multi-dimensional categories like “*<knife, cut slice, carrot>*”. These limitations hinder the study of detecting fine-grained hand actions and exploring their spatial relationship, leaving challenges in hand action detection unresolved. Therefore, establishing a large-scale benchmark with rich hand-action annotations is essential for advancing research in this field.

To this end, this paper presents a novel dataset **FHA-Kitchens**, focusing on rich and fine-grained localization and categorization information of hand actions in kitchen scenes. The FHA-Kitchens dataset encompasses a total of 2,377 video clips and 30,047 frames from eight different dish types (Figure 1(b) left). Each frame includes meticulously annotated hand action information, featuring high-quality annotations of hand interaction region boxes and corresponding coarse- and fine-grained categories. Our data were extracted from publicly available large-scale action datasets [2], focusing on videos relevant to hand actions. Subsequently, frames underwent cleaning and were annotated by ten expert voluntary annotators. To excavate more hand action information, we refined the annotation process in two aspects (Figure 1(b) right): (1) **Hand interaction regions**. These were subdivided into three sub-regions based on hand-object interaction: Left hand-Object interaction region, Right hand-Object interaction region, and Object-Object interaction region. Each sub-interaction region was annotated with bounding boxes and coarse-grained categories, denoted as “L-O”, “R-O”, and “O-O”. (2) **Hand interaction actions**. To enhance the model’s understanding of hand actions, we further refined the category of each sub-interaction region by expanding single-dimensional action categories into multi-dimensional ones, annotated in the format of triplets: *<subject, action verb, object>*, abbreviated as *<s, a, o>*, where “s-o” denotes interacting objects, and “a” represents the interaction action between the objects. Additionally, when annotating “s” and “o”, we considered the specific contact area between the interacting objects, labeled as “name_contact area” (e.g., “*carrot_end*”). Overall, we meticulously annotated **880** hand action categories (coarse- and fine-grained) for approximately 220k bounding boxes, with each category corresponding to a sub-interaction region’s localization box. Fine-grained categories per frame have nine dimensions, resulting in 877 action triplets.

Hand Action Detection (HAD) is a sub-area of Action Detection (AD) research, which has a close relation to generic object detection (OD) in the image domain. We systematically evaluated several representative AD methods [14–17] on FHA-Kitchens, observing varied performance across different levels of granularity: “Coarse-grained” and “Fine-grained”. Existing methods perform significantly worse under fine-grained labels compared to coarse-grained ones, indicating that these detection methods have a better understanding of single-dimensional coarse-grained labels (i.e., single verb or noun). However, real-world hand actions often involve both coarse-

and fine-grained information simultaneously. Therefore, exploring the impact of multi-granularity action categories in HAD tasks is both interesting and practically significant.

Among the state-of-the-art detection methods, DINO [17] showed relatively strong performance across different granularity hand actions. Building upon DINO, we propose **MG-HAD**, a novel baseline for hand action detection (HAD). MG-HAD contains a backbone, a multi-layer Transformer encoder, a multi-layer Transformer decoder, and multiple prediction branches. To better adapt to multi-granularity hand actions, we propose two novel designs: (1) **Multi-dimensional information processing**: To enhance the model’s understanding of fine-grained information, we replace the original single-dimensional content query in the decoder with multi-dimensional content queries to focus on multiple aspects of hand actions. Additionally, we introduce a Content Query Reorganization (CQR) module to generate three query sets focusing on different action dimensions as decoder inputs. (2) **Multi-granularity category processing**: We observed that the DINO’s CDN (Contrastive DeNoising) module mainly focuses on bounding boxes for contrastive denoising training, while the labels are not specially designed. To enable the model to better learn and distinguish coarse-grained and fine-grained action labels, we devise coarse-grained and fine-grained sample queries for contrastive denoising training of the labels, by adding noise to different granularity categories with specified noise positions and classes. Besides, we investigate the pre-trained ResNet50 [24] and Swin-L [25] models as backbones to extract multi-scale visual features. During training, following the DN-DETR [26] method, we add ground truth labels and boxes with noises into the Transformer decoder layers to stabilize bidirectional matching, and also adopt deformable attention [16] for improved computational efficiency.

In summary, our contributions can be summarized as follows:

- To the best of our knowledge, we are the first to study the problem of multi-granularity hand action detection and establish the first hand-action dataset **FHA-Kitchens**, which includes both hand interaction region localization and multi-granularity category annotations. This dataset can serve as a benchmark for hand action detection tasks.
- We systematically investigated the impact of different granularity hand action information in kitchen scenes on the hand action detection task and provided insights about the evaluation protocol, performance analysis, and model design.
- We propose a novel multi-granularity hand action detection method named **MG-HAD**, which is designed from the perspectives of multi-granularity and multi-dimensionality. This method incorporates Multi-dimensional Action Queries and a Coarse-Fine Contrastive Denoising module to address the mixed-grained HAD problem. MG-HAD demonstrates its effectiveness in hand action detection and could serve as a strong baseline.

2 Related work

2.1 AR & AD Dataset

Action Recognition (AR) Dataset. Existing studies on action recognition datasets can be divided into two main categories based on the types of actions: whole-body action and part-body action,

Table 1: Comparison of relevant datasets. AR: Action Recognition. AD: Action Detection. HAD: Hand Action Detection. OD: Object Detection. ACat.: Action Category. OCat.: Object Category. Dim: Action Dimension. IRBox: Interaction Region Box.

Dataset	Year	Ego	#Clip	Ave.Len	#Frame	#ACat.	#Verb	#OCat.	Dim	IRBox	Task
Whole-body action dataset											
UCF101 [1]	2012	×	13.3K	~6s	-	101	-	-	1	×	AR
ActivityNet [18]	2015	×	28K	[5,10] <i>m</i>	-	203	-	-	1	×	AR
Kinetics400 [10]	2017	×	306K	10s	-	400	359	318	2	×	AR
Kinetics600 [19]	2018	×	496K	10s	-	600	550	502	2	×	AR
Kinetics700 [20]	2019	×	650K	10s	-	700	644	591	2	×	AR
AVA [21]	2018	×	430	15 <i>m</i>	-	80	80	0	3	×	AR,AD
AVA-kinetics [22]	2020	×	230K	15 <i>m</i> ,10s	-	80	80	0	3	×	AR,AD
FineGym [23]	2020	×	32K	10 <i>m</i>	-	530	530	0	3	×	AR
Hand action dataset											
MPII cooking [3]	2012	×	5,609	15 <i>m</i>	881K	65	65	0	1	×	AR
EPIC-KITCHENS [4]	2018	✓	39.6K	3.7±5.6s	11.5M	149	125	323	2	×	AR,OD
FHA-Kitchens	2024	✓	2,377	3<i>m</i>	30,047	880	130	384	9	✓	AR,AD,HAD,OD

such as UCF101 [1], Kinetics [10, 19, 20], ActivityNet [18], FineGym [23], and others [27–33]. These datasets primarily focus on whole-body actions, lacking fine-grained action information from specific body parts. Datasets like MPII Cooking Activities [3] and EPIC-KITCHENS [4] refine the action verb part and consider interacting objects, yet they do not describe the localization of action interaction regions or the relationships between interacting objects, crucial for HAD tasks.

Action Detection (AD) Dataset. Compared to action recognition datasets, fewer datasets are available for action detection [21, 22]. This is due to the need to annotate the position and category of each action instance, which requires more effort for dataset construction. The AVA dataset [21] focuses on human action localization, providing bounding box annotations for each person. However, this dataset primarily focuses on whole-body actions, providing location information for individuals rather than action interaction regions. Moreover, the provided action categories are mainly single-dimensional coarse-grained verbs (*e.g.*, “*sit*”, “*write*”, and “*stand*”). FHA-Kitchens dataset addresses these limitations by providing precise bounding box annotations for each hand sub-interaction region. A comprehensive comparison between FHA-kitchens and existing datasets is presented in Table 1. In contrast to existing datasets, (1) We provide precise localization information by meticulously annotating hand interaction regions and corresponding interaction objects using bounding boxes. (2) We offer two granularity for hand actions: coarse- and fine-grained. For fine-grained categories, we use multi-dimensional triplets to represent each sub-interaction region action, expanding the dimensionality of each frame to 9. (3) We not only focus on the interacting objects that generate interaction actions but also consider the active and passive relationships between these objects, capturing their contact areas.

2.2 AR & AD Method

Action Recognition (AR) Method. Existing action recognition methods can be broadly summarized into two pipelines based on technical approaches. The first pipeline employs a 2D CNN [34–37] to learn frame-level semantics and then aggregate them temporally using 1D modules. For example, TSN [11] divides an action instance into multiple segments, represents it with a sparse sampling scheme,

and applies average pooling to fuse predictions from each frame. TRN [38] and TSM [39] replace pooling with temporal reasoning and shift modules, respectively. The second pipeline directly utilizes a 3D CNN [10, 12, 13, 40–42] to capture spatial-temporal semantics, such as I3D [10], SlowFast [12], and Video Swin Transformer [13]. On the other hand, AR methods can be categorized into coarse-grained [43, 44] and fine-grained [45–48] based on the granularity of the actions.

Action Detection (AD) Method. Most state-of-the-art action detection methods [12, 49–52] commonly follow a two-stage pipeline, utilizing separate 2D and 3D backbones for localization and video feature extraction, respectively. Since transformer [53] was introduced for machine translation, it has become a widely adopted backbone for sequence-to-sequence tasks [17, 54–57]. Most recent methods [58–63] utilize a unified backbone to perform action detection. VAT [58] is a transformer-style action detector designed to aggregate spatiotemporal context around target actors. EVAD [60], built upon the ViT framework, offers an end-to-end efficient video action detection method. WOO [61] and TubeR [62] are query-based action detectors that follow the detection frameworks of [64, 65] to predict bounding boxes and action classes, while STMixer [63] is a one-stage query-based detector that adaptively samples discriminative features. However, we observed that these methods primarily focus on individual human actions and overlook action interaction regions, interacting objects, and their relationships. Leveraging the advantages of transformer-based detection models, we propose an end-to-end solution capable of simultaneous hand action localization and recognition.

3 FHA-Kitchens Dataset

3.1 Data Collection And Organization

Data Collection. The proposed dataset is derived from the large-scale action dataset Kinetics 700_2020 [2], which comprises approximately 650K YouTube video clips and over 700 action categories. To narrow our focus to hand actions, we performed filtering and processing operations on the original videos in three steps. (1) Content Localization: We observed that videos in kitchen scenes prominently showcase human hands. So we sought out and extracted relevant videos set against a kitchen backdrop. (2) Quality Selection:

To ensure dataset quality, we selectively chose videos with higher resolutions. Specifically, 87% of the videos were recorded at $1,280 \times 720$ resolution, while another 13% had a shorter side of 480. Additionally, 67% of the videos were captured at 30 frames per second (fps), and another 33% were recorded at 24~25 fps. (3) **Duration Control**: We imposed a duration constraint on the videos, ranging from 30 seconds to 5 minutes, to exclude excessively long videos. This constraint aimed to maintain a balanced distribution within the sample space. Finally, we collected a total of 2,377 video clips, amounting to 84.22 minutes of footage, encompassing 8 distinct types of dishes.

Data Organization. The collected video data was reorganized and cleaned to align with our annotation criteria (Section 3.2). At last, we obtained a total of 30,047 high-quality candidate video frames containing diverse hand actions for the FHA-Kitchens dataset. Compared to the initial collection, 113,436 frames were discarded during the cleaning process.

3.2 Data Annotation

We recruited 10 voluntary annotators to annotate hand actions for each frame with high quality, including bounding boxes and action categories. The annotation content and criteria are detailed below.

Bounding Box Annotation: We annotated the bounding boxes for both interaction regions (IR) and interaction objects (IO). (1) **IR**: We divided the hand's interaction region into three sub-interaction regions: Left hand-Object (L-O), Right hand-Object (R-O), and Object-Object (O-O) interaction regions (Figure 1(b) middle), representing regions where the left hand directly contacts an object, the right hand directly contacts an object, and objects interact with each other, respectively. The reason for focusing on O-O is that interactions between objects also involve the participation of hands. (2) **IO**: To better understand interaction actions, we also annotated the interactive object pair within each sub-interaction region using bounding boxes. For example, in L-O, we annotated objects directly touched by the left hand. In O-O, we annotated the interacting objects directly involved in hand actions (e.g., *utility knife* and *carrot*). However, during annotation, we may encounter overlapping bounding boxes, i.e., the same interacting object will satisfy two annotation definitions, for example, the *utility knife* in Figure 1, which is both the object directly touched by the right hand in the R-O and the active force provider in the O-O. In this case, we annotate all the labels because the same object participates in different interaction actions and has different roles (Annotation details can be seen in *supplementary material*). Finally, we annotated a total of 198,839 bounding boxes, including 49,746 hand boxes, 66,402 interaction region boxes, and 82,691 interaction object boxes.

Hand Action Annotation: We annotated coarse- and fine-grained action categories for each sub-interaction region. Coarse-grained categories, denoted by the generic terms “L-O”, “R-O”, and “O-O”, represent the coarse actions within the sub-interaction regions. Different from existing fine-grained datasets. We annotate each fine-grained action category in a triplet format: *<subject, action verb, object>*. (1) **Subject & Object**: We considered the “active-passive” relationship between objects, where the “subject” refers to the active force provider (e.g., *utility knife*) and the “object” refers to the passive force receiver (e.g., *carrot*), and annotate them in

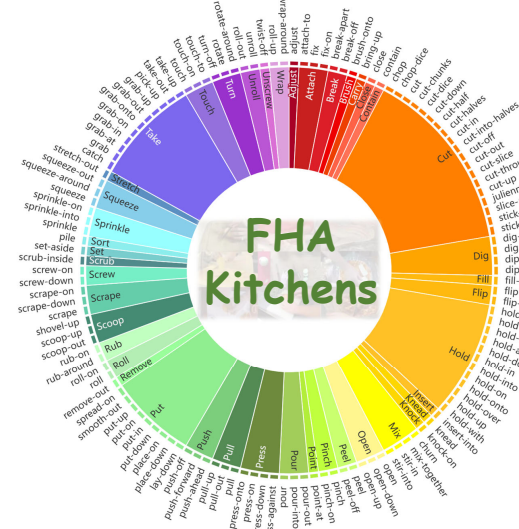


Figure 2: An overview of the action verbs and their parent action categories in FHA-Kitchens.

order within the action triplet. In L-O or R-O, the subject represents the corresponding hand, while the object denotes the directly interacting object. Furthermore, to enrich the description of each action, we also considered the contact areas of interacting objects within each sub-interaction region. For example, as shown in the first green block in the middle of Figure 1(b), we labeled the subject as “*hand_left*” and the object as “*carrot_end*”. We referred to the EPIC-KITCHENS [4] dataset to define the object noun. (2) **Action Verb**: It describes the fine-grained hand action within the sub-interaction region. We used fine-grained verbs in the annotated action triplets and constructed the verb vocabulary by sourcing from EPIC-KITCHENS [4], AVA [21], and Kinetics 700 [20].

3.3 Statistics of the FHA-Kitchens Dataset

Overview of FHA-Kitchens. As summarized in Table 1, we annotated hand action information for 30,047 frames from 2,377 clips, resulting in 880 action categories (including 877 action triplets), 130 action verbs, and 384 interaction object nouns. We have taken steps to refine the dataset by focusing on hand action categories and interaction regions, providing more precise localization bounding boxes and rich hand action categories for the three sub-interaction regions. Compared to the original action annotations in Kinetics 700_2020 [2], the FHA-Kitchens dataset expands the action labels by 7 dimensions, increases the number of action categories by 52 times, and introduces 122 new action verbs. Furthermore, we provide bounding boxes for hand action regions (i.e., 66,402 interaction region boxes). This expansion significantly enhances the diversity of hand action annotations, provides valuable region-level contextual information for each action, and facilitates future research for a wider range of video understanding tasks. The FHA-Kitchens dataset is then randomly divided into the disjoint train, validation, and test sets, with a video clip-based ratio of 7:1:2.

Annotation Statistics. Our annotation primarily focuses on hand interaction regions, interaction objects, and their corresponding interaction actions, resulting in a diverse array of verbs, nouns, and bounding boxes. Following the fine-grained annotation principles [4], we ensured minimal semantic overlap among action verb-noun categories, rendering them suitable for multi-category action recognition and detection. **(1) Verbs:** The annotated dataset comprises 130 action verbs that have been grouped into 43 parent verb categories (Figure 2 and Figure 3). The three most prevalent parent verb categories, based on the count of sub-action verbs, are *Cut*, *Hold*, and *Take*, representing the most frequently occurring hand actions in kitchen scenes. Figure 3 visually depicts the distribution of all verb categories within FHA-Kitchens, ensuring the presence of at least one instance for each verb category. **(2) Nouns:** In the annotation process, we identified a total of 384 interaction object noun categories that are associated with actions, categorized into 17 super-categories. Figure 4 shows the distribution of noun categories based on their affiliations with super-categories. Notably, the super-category “vegetables & plants” exhibits the highest number of sub-categories, followed by “kitchenware”, which aligns with typical kitchen scenes. **(3) Bounding Boxes:** We performed a comprehensive statistical analysis on the bounding boxes of the three sub-interaction regions and the corresponding interaction objects. Specifically, we focused on two aspects: the box area and the aspect ratio. Details can be found in *supplementary material*.



Figure 3: The distribution of instances per action verb category (the outer ring in Figure 2) in the FHA-Kitchens dataset.

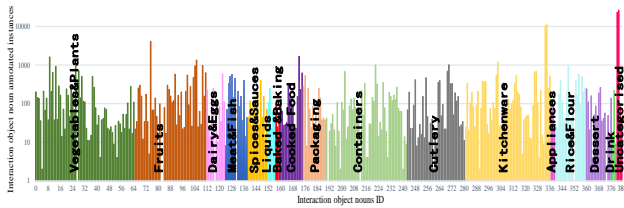


Figure 4: The distribution of instances per object noun category from 17 super-categories in the FHA-Kitchens dataset.

3.4 Benchmark Setup

Methods. We benchmark several representative action recognition methods [11–13, 55, 66] and detection methods [14–17] with different backbone networks on the proposed FHA-Kitchens dataset based on the MMAAction2 [67] and MMDetection [68] codebases. We establish three tracks using the provided dataset. **SL-AD Track:** The aim is to evaluate the supervised learning performance of different detection models on hand interaction regions with different

Table 2: Detection results (mAP) of hand interaction regions with different granularity levels of action categories using different methods, i.e., Faster-RCNN, YOLOX, Deformable DETR, and DINO on the validation set of the SL-D track.

Method	Backbone	Granularity levels	
		Coarse-Grained	Fine-Grained
Faster-RCNN [14]	R-50	65.2	48.5
	R-101	66.1	50.0
YOLOX [15]	YOLOX-s	71.8	46.9
	YOLOX-x	75.6	49.8
Deformable DETR [16]	R-50	73.0	52.4
DINO [17]	R-50	75.2	53.5

granularity levels of action categories. The results of the methods are shown in Table 2. **SL-AR Track:** This track primarily evaluates the supervised learning performance of different action recognition models on fine-grained hand actions. We trained the models with and without pre-trained weights on the FHA-Kitchens dataset. **DG Track:** It focuses on experiments for Intra- and Inter-class Domain Generalization in Interaction Region Detection, exploring both intra-class and inter-class perspectives. All models on the SL-AD, SL-AR, and DG tracks were trained and tested using NVIDIA GeForce RTX 3090 GPUs. For the SL-AD and DG tracks, we employ the mean Average Precision (mAP) [69] as the primary evaluation metric, while for the SL-AR track, Top-1 accuracy and Top-5 accuracy (%) are adopted. Detailed results of SL-AR and DG can be found in *supplementary material*.

Results and Discussion. The results in Table 2 show that current detection methods perform well in learning single-dimensional coarse-grained categories like verbs or nouns. However, they struggle in learning multi-dimensional fine-grained action categories. Understanding the intricate nature of real-world hand actions, which encompass both coarse- and fine-grained information, underscores the significance of investigating multi-granularity action categories in HAD tasks, an area that poses significant challenges and remains largely unexplored. To fill this gap, we propose a novel method for multi-granularity hand action detection.

4 A Simple Yet Strong Baseline

4.1 A Multi-Granularity Framework

Drawing inspiration from the image-based DINO [17], we propose the novel MG-HAD method with specific novel designs in the decoder for multi-granularity hand action detection (Figure 5). MG-HAD consists of a backbone, a multi-layer Transformer encoder, a multi-layer Transformer decoder, and multiple prediction branch heads. Given a video clip, for each frame, we utilize backbones like ResNet [24] or Swin Transformer [25] to extract multi-scale features, which are then fed into the Transformer encoder along with corresponding positional embeddings. After enhancing features through the encoder layers, we initialize anchors as positional queries for the decoder using a mixed query selection strategy, following the design of DINO, without initializing content queries but leaving them learnable. It’s worth noting that the original content queries focus on semantic information of single-dimensional categories, which is not suitable for fine-grained multi-dimensional

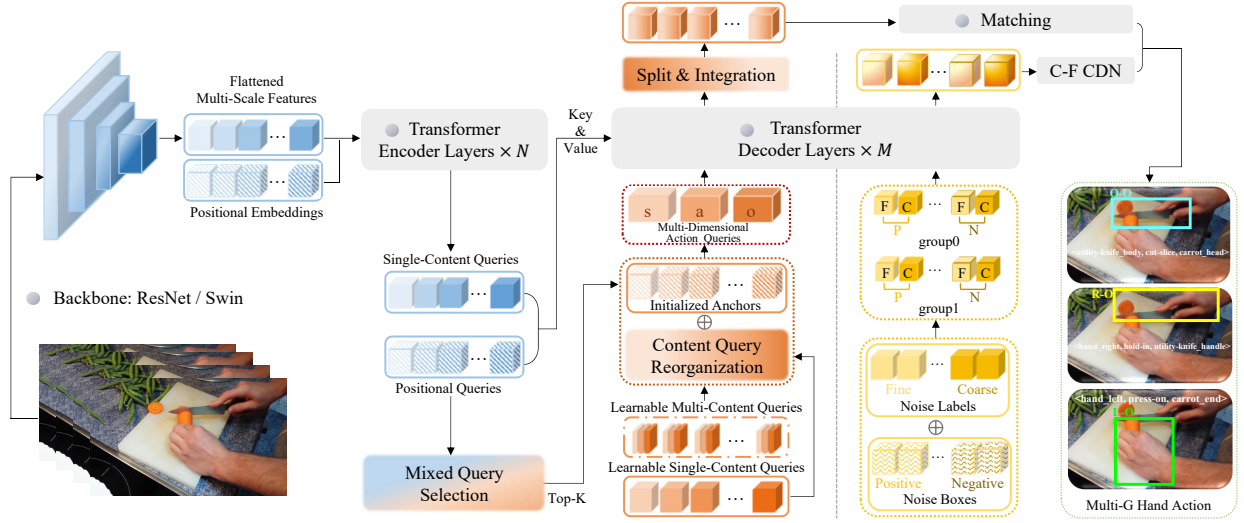


Figure 5: The overall architecture of MG-HAD, a novel end-to-end hand action detection model based on DINO [17]. The improvements mainly focus on the decoder part. Specifically, (1) we introduce a new design for the content query part, transforming the original single-dimensional content queries into multi-dimensional ones. They are further processed by the designed CQR module, combined with initialized anchors, and inputted into the decoder. The outputted three query sets with different action dimensions go through the Split & Integration module to generate N queries containing three action dimensions. Finally, the matching process is conducted to predict hand action results (see Section 4.2); (2) we introduce a C-F CDN training approach, which involves adding coarse- and fine-grained noise to labels to generate four types of CDN queries for contrastive denoising training (see Section 4.3). F: Fine-grained, C: Coarse-grained, Multi-G: Multi-granularity.

categories in the new task. Therefore, we modify the single-content query to multi-content queries and introduce a Content Query Reorganization (CQR) module to obtain query sets focusing on three different sub-action dimensions, as detailed in Section 4.2. Additionally, similar to DINO, we have an extra CDN branch to perform contrastive denoising training. In contrast to the standard CDN method, we specifically devise a novel coarse-fine granularity contrastive denoising training approach to distinguish labels with different granularity levels, which will be discussed in Section 4.3.

4.2 Multi-Dimensional Action Queries

Comparing the results presented in Table 2, it's clear that existing detection methods struggle with learning from multi-dimensional fine-grained labels. Fine-grained hand action detection poses a greater challenge compared to coarse-grained detection due to the need to discern subtle differences in similar hand actions. Additionally, multi-dimensional fine-grained labels provide important supervisory signals about subject, object, and action categories, as well as localization information. However, effectively encoding this information at different dimensions and leveraging these supervisory signals, particularly in terms of query design within the DETR series framework [16, 17, 65], remains unexplored.

Implementation: We observed that the current design of content queries mainly focuses on single-dimensional semantic information, *i.e.*, single verb or noun categories. However, in fine-grained categories, we incorporate both verb and noun categories, generating multi-dimensional semantic information, *i.e.*, $\langle c_1, c_2, c_3 \rangle$ ($c_1, c_3 \in \text{nouns}$, and $c_2 \in \text{verbs}$), or more specific $\langle s, a, o \rangle$. If we stick to the

original design, content queries would consider $\langle s, a, o \rangle$ as a whole, learning global information from a single-dimensional perspective. To enhance the model's focus on local information of sub-categories, we transform a set of content queries $Q = \{q_1, \dots, q_n\}$ originally focusing on single dimensions into three sets of content queries, *i.e.*, Q_s , Q_a , and Q_o , focusing on different action dimensions. n is the index of the original queries. Specifically, we first convert each query element q_n (bottom orange cubes in Figure 5) into three sub-queries, *i.e.*, q_{n_s} , q_{n_a} , and q_{n_o} , expanding N original queries to $3 \times N$ sub-queries. Next, through our designed Content Query Reorganization (CQR) module, sub-queries focusing on the same action dimension (*i.e.*, $q_{1_s}, q_{2_s}, \dots, q_{n_s}$) are selected and reorganized to obtain a query set for each action dimension. Additionally, to ensure a comprehensive understanding of fine-grained categories, we introduce an action dimensional hyper-parameter w_d ($d \in \{s, a, o\}$), to add a certain proportion of weight to each query set, which is then sum with the global information (*i.e.*, $Q = \{q_1, \dots, q_n\}$). This process is formulated as:

$$Q_d = \text{CQR}(\{q_{nd}\}_{n=1}^N) = \sum_{n=1}^N q_{nd} \times w_d + Q, \quad d = s, a, \text{ or } o. \quad (1)$$

After passing through the CQR module, we obtain content query sets for the three action dimensions. These sets are then summed with the initialized anchors to yield multi-dimensional action queries. Each dimensional query set has a length of N , resulting in a total length of $3N$. Following the decoder layers, three query sets for different action dimensions (Q'_s , Q'_a , and Q'_o) are outputted.

Subsequently, through the Split&Integration module, queries from different action dimensions with the same index (e.g., q_{1s}, q_{1a}, q_{1o}) are integrated to generate N queries, each of which contains information from three action dimensions (*top orange cubes in Figure 5*):

$$\{q_n\}_{n=1}^N = SI(Q'_s, Q'_a, Q'_o) = \{q_{n_s} + q_{n_a} + q_{n_o}\}_{n=1}^N, \quad (2)$$

where SI represents the Split&Integration module. Finally, the matching process is conducted to predict hand action results.

Analysis: In our design of multi-dimensional action queries, we introduce an action dimensional hyper-parameter w_d ($d \in \{s, a, o\}$), to control the proportion of local information (sub-categories) fused with global information (triplet categories). In the three action dimensions $\langle s, a, o \rangle$, the a dimension is the most crucial for our task. Therefore, we use w_a as the central weight to dynamically adjust the weight proportions of the three action dimensions, with a total sum of 1. To determine the optimal weight distribution, we conducted a total of 10 comparative experiments under different backbones, with detailed results provided in *supplement material*.

4.3 Coarse-Fine Contrastive Denoising

For object detection, DINO is highly effective in stabilizing training and accelerating convergence. With the help of DN queries, it learns to predict “no object” for anchors without nearby objects, thereby inhibiting confusion and selecting high-quality anchors (queries) for predicting bounding boxes. However, in HAD tasks where hand action categories may overlap or be similar, DINO primarily addresses the confusion of boxes but overlooks label categories, resulting in poor prediction capability for different granularity levels of hand action categories. To address this issue, we propose a Coarse-Fine granularity Contrastive DeNoising (C-F CDN) training approach to reject anchors with “incorrect granularity labels”.

Implementation: DINO introduces two hyper-parameters γ_1 and γ_2 , to control the scale of box and label noise, respectively. The generated noises are no larger than γ_1 and γ_2 , aiming to enable the model to reconstruct the ground truth (GT) from moderately noisy queries. We observed that DINO only designs two types of CDN queries for the box: positive and negative queries, while the label is set to be randomly generated. In the proposed method, while keeping the box settings unchanged, we further generate two types of CDN queries for the label: coarse-grained and fine-grained queries (*dark and light yellow cubes in Figure 5*). Moreover, unlike the strategy of randomly generating noisy labels, we add noise by specifying the noise position and noise category for different granularity labels. Specifically, coarse-grained queries add noise containing fine-grained information, while fine-grained queries add noise containing coarse-grained information, with the expectation of predicting the correct granularity label for each GT box. In Figure 5, each CDN group comprises four types of queries: positive-coarse, positive-fine, negative-coarse, and negative-fine. If a frame has n GT bounding boxes, a CDN group will contain 4 types of $2 \times n$ queries. Similar to DINO, we also utilize multiple CDN groups to enhance the effectiveness of the method. The reconstruction loss for bounding box regression includes l_1 and GIOU losses, while focal loss [70] is employed for classification.

Analysis: When designing the noise label generation strategy, we replaced the “random” generation of noise with “specified”, reducing randomness by specifying noise positions and categories.

Table 3: Results for MG-HAD and other DETR Series detection models with the ResNet50 backbone on the FHA-Kitchens validation set trained with 12 epochs. M-G: Mixed-Grained, C-G: Coarse-Grained, F-G: Fine-Grained.

Method	FHA-Kitchens val mAP(%)		
	M-G label	C-G sub-label	F-G sub-label
DETR [65]	42.3	72.8	41.9
Deformable DETR [16]	49.4	70.9	49.1
DAB-DETR [71]	52.1	73.1	51.8
DDQ-4scale [72]	53.8	67.8	53.7
DINO-4scale [17]	54.7	76.3	54.5
MG-HAD-4scale	57.0(+2.3)	75.6	56.8(+2.3)

This ensures noise is added to different granularity labels, generating CDN queries encompassing various granularity. To determine the optimal setting, we considered the noise distribution of different granularity categories in real-world scenarios and ensured contrastive learning between coarse and fine-grained information. We conducted three sets of comparative experiments (Details can be found in *supplementary material*). The final selected setting, as shown in Eq. (5), exhibits the most significant improvement. Hence, subsequent experiments were conducted using this setting for further investigation. Our method’s success lies in its ability to suppress confusion at the category level and select appropriate granularity to predict hand action categories, thus enhancing its ability to predict multi-granularity information.

$$\text{noise label} = \begin{cases} \text{fine-grained} & i \in [0, 3) \\ \text{mixed-grained} & i \in [3, C) \end{cases}, \quad (3)$$

where i indexes the multi-granularity action category for a specific instance (i.e., 0~2 denote coarse-grained categories while 3~C-1 denote fine-grained categories), and C is the number of categories. “fine-grained” and “mixed-grained” denote that the noise label is chosen randomly from the fine-grained categories and the combination of the coarse-grained and fine-grained categories, respectively.

5 Experiments

5.1 Experiments Settings

Dataset and Metric. Due to the absence of benchmarks for this new task, we evaluated our model and other representative detection models solely on the FHA-Kitchens dataset. We conducted experiments using two different backbones: ResNet-50 [24] pre-trained on ImageNet-1k [73] and Swin-L [25] pre-trained on ImageNet-22k [73]. All detection models utilize pre-trained weights on the MS COCO object detection dataset [69]. Furthermore, we not only report the overall validation results using mixed-grained labels but also separately report the validation results for coarse-grained and fine-grained sub-labels. We follow previous works and adopt mean Average Precision (mAP) [69] as the primary evaluation metric.

Implementation Details. We trained the MG-HAD model on the FHA-Kitchen dataset using the MMDetection [68] codebase. Specifically, we utilized pre-trained weights on the MS COCO [69] object detection dataset and fine-tuned it on the hand action detection task on FHA-Kitchens. We trained the model under two different settings: 4scale-R-50 and 5scale-Swin-L. Following DINO [17],

Table 4: Results of MG-HAD and other SOTA detection models on the FHA-Kitchens validation set. R-50: ResNet-50, M-G: Mixed-Grained, C-G: Coarse-Grained, F-G: Fine-Grained.

Method	Epoch	Backbone	FHA-Kitchens val mAP(%)		
			M-G label	C-G sub-label	F-G sub-label
<i>Faster R-CNN</i> [14]	108	R-50	48.3	22.3	48.6
<i>YOLOX</i> [15]	100	YOLOX-x	50.7	70.8	50.5
<i>DETR</i> [65]	150	R-50	50.6	73.1	50.3
<i>Deformable DETR</i> [16]	50	R-50	53.7	72.6	53.4
<i>DAB-DETR</i> [71]	50	R-50	54.7	75.2	54.5
<i>DINO-4scale</i> [17]	24	R-50	56.3	74.5	56.0
<i>DINO-4scale</i> [17]	12	R-50	54.7	76.3	54.5
<i>DINO-5scale</i> [17]	12	Swin-L	56.3	76.3	56.1
MG-HAD-4scale	24	R-50	57.7(+1.4)	75.3	57.5(+1.5)
	12		57.0(+2.3)	75.6	56.8(+2.3)
MG-HAD-5scale	12	Swin-L	59.4(+3.1)	77.6	59.2(+3.1)

we used the Adam optimizer [74] for model training, with an initial learning rate of 1×10^{-4} and weight decay is 10^{-4} . The experiments were conducted on the NVIDIA GeForce RTX 3090 GPUs, with a batch size of 2 for 4scale-R-50 and 1 for 5scale-Swin-L. By default, MG-HAD was trained for 12 epochs, taking approximately 5 hours. More details are provided in the *supplement material*.

5.2 Main Results

12-Epoch Setting. To demonstrate the effectiveness of our method for the multi-granularity HAD task, we compared it with representative strong baselines from the DETR series [16, 17, 65, 71, 72] on the FHA-Kitchens dataset under the setting of ResNet-50 backbone and 12 epochs. In particular, our method, DINO [17], and DDQ [72] mainly report results under the 4scale setting. As shown in Table 3, our method achieves much better accuracy in detecting mixed-grained hand actions, owing to the proposed C-F CDN module and multi-dimensional action queries. Specifically, it achieves an improvement of **+2.3** AP on mixed-grained labels compared to the current strongest baseline DINO [17] under the same setting. Furthermore, compared to the classic DETR [65], our method achieves a significant improvement of **+14.7** AP. Note that our method not only performs well for mixed-grained labels but also shows improvement in the validation results for fine-grained sub-labels.

Comparison with SOTA Detection Methods. To comprehensively and fairly validate the effectiveness of our method in enhancing the performance of multi-granularity hand actions, we compared it with other state-of-the-art (SOTA) detection methods on the FHA-Kitchens dataset, utilizing their optimal settings (refer to the MMDetection [68] codebase). DINO exhibits relatively fast convergence, achieving good results with just 12 epochs on the Swin-L backbone. Our method inherits the convergence capability of DINO but yields more significant improvements. We adopted the same settings as DINO [17], utilizing both 4scale ResNet-50 and 5scale Swin-L backbones, trained for 12 epochs and 24 (2×) epochs, respectively. The results in Table 4 indicate the following: (1) Our method exhibits a significant improvement compared to the baseline [17], which can be attributed to the design of handling fine-grained information in our model; (2) Comparing models trained for 24 epochs and 12 epochs, the main improvement lies in the accuracy of fine-grained action detection. Since the FHA-Kitchens

Table 5: Ablation study of the key components in MG-HAD. C-F CDN: Coarse-Fine granularity Contrastive De-Noising Training, Multi-DA Q: Multi-Dimensional Action Queries.

Method	Algorithm Components		mAP(%)	
	C-F CDN	Multi-DA Q	4scale-R-50	5scale-Swin-L
Baseline [17]			54.7	56.3
MG-HAD	✓		56.6	58.2
		✓	56.4	58.7
	✓	✓	57.0	59.4

dataset contains overwhelming fine-grained categories over the coarse-grained ones, the model’s representation capacity may be primarily utilized for fitting fine-grained categories; (3) Under the 5-scale Swin-L backbone, our method achieves a significant improvement of **59.4** AP for mixed-grained hand actions with just 12 epochs. This indicates that using a more powerful backbone [25] can improve both coarse- and fine-grained action detection accuracy. Specifically, the detection accuracy of fine-grained actions is increased by **+3.1** AP and the detection accuracy of coarse-grained actions is increased by **+1.3** AP. The visualization of the detection results can be found in the *supplement material*.

5.3 Ablation Studies

Effectiveness of New Components: Our method utilizes the multi-dimensional action queries for multi-dimensional information processing, as introduced in Section 4.2, and the C-F CDN module for multi-granularity information processing, as described in Section 4.3. To further validate the effectiveness of these components, we separately isolated them from the model and evaluated the performance under two settings: 4scale ResNet-50 and 5scale Swin-L, as shown in Table 5, where the baseline denotes the original design proposed by DINO [17]. As can be seen, while the strong baseline DINO [17] has already surpassed previous models, the proposed MG-HAD introduces two novel designs that notably boost performance in hand action detection. Each module significantly enhances the baseline on both backbones, and their combined effect further enhances performance, demonstrating their complementary role in understanding multi-granularity hand action information.

6 Conclusion

In this paper, we present the first study on multi-granularity hand action detection, aiming to understand the diverse hand actions through localizing regions and recognizing various granularity categories of hand actions. We establish **FHA-Kitchens**, the first fine-grained hand action detection dataset, comprising 30,047 high-quality video frames, 198,839 bounding boxes, and 880 hand action categories. Through systematic evaluation, we identify that existing detection methods excel in coarse-grained actions but struggle with fine-grained ones. To address this, we propose **MG-HAD**, a simple yet strong baseline model leveraging the Transformer detector with two novel designs. It outperforms previous methods across various granularities of hand actions. FHA-Kitchens and MG-HAD can serve as a valuable testbed and baseline for future research.

ACKNOWLEDGMENTS

This work was supported in part by the National Key Research and Development Program of China under No. 2021YFC3300200, the National Natural Science Foundation of China (Grant No. 62276195), and the Special Fund of Hubei LuoJia Laboratory under Grant 220100014. The numerical calculations in this paper were done using the supercomputing system at the Supercomputing Center of Wuhan University. We also thank all the volunteers who contributed to the dataset.

References

- [1] Khurram Soomro, Amir Roshan Zamir, and Mubarak Shah. Ucf101: A dataset of 101 human actions classes from videos in the wild. In *Proceedings of the IEEE Conference on Computer Vision and Pattern Recognition*, 2012.
- [2] Lucas Smaira, João Carreira, Eric Noland, Ellen Clancy, Amy Wu, and Andrew Zisserman. A short note on the kinetics-700-2020 human action dataset. *arXiv preprint arXiv:2010.10864*, 2020.
- [3] Marcus Rohrbach, Sikandar Amin, Mykhaylo Andriluka, and Bernt Schiele. A database for fine grained activity detection of cooking activities. In *Proceedings of the IEEE Conference on Computer Vision and Pattern Recognition*, pages 1194–1201. IEEE, 2012.
- [4] Dima Damen, Hazel Doughty, Giovanni Maria Farinella, Sanja Fidler, Antonino Furnari, Evangelos Kazakos, Davide Moltisanti, Jonathan Munro, Toby Perrett, Will Price, et al. Scaling egocentric vision: The epic-kitchens dataset. In *Proceedings of the European Conference on Computer Vision*, pages 720–736, 2018.
- [5] Jing Zhang and Dacheng Tao. Empowering things with intelligence: A survey of the progress, challenges, and opportunities in artificial intelligence of things. *IEEE Internet of Things Journal*, 8(10):7789–7817, 2020.
- [6] Hezhen Hu, Weilun Wang, Wengang Zhou, and Houqiang Li. Hand-object interaction image generation. *Advances in Neural Information Processing Systems*, 35:23805–23817, 2022.
- [7] Chengshu Li, Ruohan Zhang, Josiah Wong, Cem Gokmen, Sanjana Srivastava, Roberto Martin-Martin, Chen Wang, Gabriel Levine, Michael Lingelbach, Jiankai Sun, et al. Behavior-1k: A benchmark for embodied ai with 1,000 everyday activities and realistic simulation. In *Conference on Robot Learning*, pages 80–93. Proceedings of Machine Learning Research, 2023.
- [8] G. Palli, S. Pirozzi, C. Natale, G. De Maria, and C. Melchiorri. Mechatronic design of innovative robot hands: Integration and control issues. In *Proceedings of the IEEE/ASME International Conference on Advanced Intelligent Mechatronics*, pages 1755–1760, 2013.
- [9] Ruolin Ye, Wengqiang Xu, Haoyuan Fu, Rajat Kumar Jenamani, Vy Nguyen, Cewu Lu, Katherine Dimitropoulou, and Tapomayukh Bhattacharjee. Rcare world: A human-centric simulation world for caregiving robots. In *Proceedings of the IEEE International Conference on Intelligent Robots and Systems*, pages 33–40. IEEE, 2022.
- [10] Joao Carreira and Andrew Zisserman. Quo vadis, action recognition? a new model and the kinetics dataset. In *Proceedings of the IEEE Conference on Computer Vision and Pattern Recognition*, pages 6299–6308, 2017.
- [11] Limin Wang, Yuanjun Xiong, Zhe Wang, Yu Qiao, Dahua Lin, Xiaoou Tang, and Luc Van Gool. Temporal segment networks: Towards good practices for deep action recognition. In *Proceedings of the European Conference on Computer Vision*, pages 20–36. Springer, 2016.
- [12] Christoph Feichtenhofer, Haoqi Fan, Jitendra Malik, and Kaiming He. Slowfast networks for video recognition. In *Proceedings of the IEEE International Conference on Computer Vision*, pages 6202–6211, 2019.
- [13] Ze Liu, Jia Ning, Yue Cao, Yixuan Wei, Zheng Zhang, Stephen Lin, and Han Hu. Video swin transformer. In *Proceedings of the IEEE Conference on Computer Vision and Pattern Recognition*, pages 3202–3211, 2022.
- [14] Shaoqing Ren, Kaiming He, Ross Girshick, and Jian Sun. Faster r-cnn: Towards real-time object detection with region proposal networks. *Advances in Neural Information Processing Systems*, 28, 2015.
- [15] Zheng Ge, Songtao Liu, Feng Wang, Zeming Li, and Jian Sun. Yolox: Exceeding yolo series in 2021. In *Proceedings of the IEEE Conference on Computer Vision and Pattern Recognition*, 2021.
- [16] Xizhou Zhu, Weijie Su, Lewei Lu, Bin Li, Xiaogang Wang, and Jifeng Dai. Deformable detr: Deformable transformers for end-to-end object detection. In *Proceedings of the International Conference on Learning Representations*, 2021.
- [17] Hao Zhang, Feng Li, Shilong Liu, Lei Zhang, Hang Su, Jun Zhu, Lionel M Ni, and Heung-Yeung Shum. Dino: Detr with improved denoising anchor boxes for end-to-end object detection. In *Proceedings of the International Conference on Learning Representations*, 2023.
- [18] Fabian Caba Heilbron, Victor Escorcia, Bernard Ghanem, and Juan Carlos Nibbles. Activitynet: A large-scale video benchmark for human activity understanding. In *Proceedings of the IEEE Conference on Computer Vision and Pattern Recognition*, pages 961–970. IEEE, 2015.
- [19] Joao Carreira, Eric Noland, Andras Banki-Horvath, Chloe Hillier, and Andrew Zisserman. A short note about kinetics-600. In *Proceedings of the IEEE Conference on Computer Vision and Pattern Recognition*, 2018.
- [20] Joao Carreira, Eric Noland, Chloe Hillier, and Andrew Zisserman. A short note on the kinetics-700 human action dataset. In *Proceedings of the IEEE Conference on Computer Vision and Pattern Recognition*, 2019.
- [21] Chunhui Gu, Chen Sun, David A Ross, Carl Vondrick, Caroline Pantofaru, Yeqing Li, Sudheendra Vijayanarasimhan, George Toderici, Susanna Ricco, Rahul Sukthankar, et al. Ava: A video dataset of spatio-temporally localized atomic visual actions. In *Proceedings of the IEEE Conference on Computer Vision and Pattern Recognition (challenge)*, pages 6047–6056, 2018.
- [22] Ang Li, Meghana Thotakuri, David A Ross, João Carreira, Alexander Vostrikov, and Andrew Zisserman. The ava-kinetics localized human actions video dataset. In *Proceedings of the IEEE Conference on Computer Vision and Pattern Recognition (challenge)*, 2020.
- [23] Dian Shao, Yue Zhao, Bo Dai, and Dahua Lin. Finegym: A hierarchical video dataset for fine-grained action understanding. In *Proceedings of the IEEE Conference on Computer Vision and Pattern Recognition*, pages 2616–2625, 2020.
- [24] Kaiming He, Xiangyu Zhang, Shaoqing Ren, and Jian Sun. Deep residual learning for image recognition. In *Proceedings of the IEEE Conference on Computer Vision and Pattern Recognition*, pages 770–778, 2016.
- [25] Ze Liu, Yutong Lin, Yue Cao, Han Hu, Yixuan Wei, Zheng Zhang, Stephen Lin, and Baining Guo. Swin transformer: Hierarchical vision transformer using shifted windows. In *Proceedings of the IEEE International Conference on Computer Vision*, pages 10012–10022, 2021.
- [26] Feng Li, Hao Zhang, Shilong Liu, Jian Guo, Lionel M Ni, and Lei Zhang. Dn-detr: Accelerate detr training by introducing query denoising. In *Proceedings of the IEEE Conference on Computer Vision and Pattern Recognition*, pages 13619–13627, 2022.
- [27] Mathew Monfort, Alex Andonian, Bolei Zhou, Kandan Ramakrishnan, Sarah Adel Bargal, Tom Yan, Lisa Brown, Quanfu Fan, Dan Gutfreund, Carl Vondrick, et al. Moments in time dataset: One million videos for event understanding. *IEEE Transactions on Pattern Analysis and Machine Intelligence*, 42(2):502–508, 2019.
- [28] Fabian Caba Heilbron, Joon-Young Lee, Hailin Jin, and Bernard Ghanem. What do i annotate next? an empirical study of active learning for action localization. In *Proceedings of the European Conference on Computer Vision*, pages 199–216, 2018.
- [29] Hueihan Jhuang, Juergen Gall, Silvia Zuffi, Cordelia Schmid, and Michael J Black. Towards understanding action recognition. In *Proceedings of the IEEE International Conference on Computer Vision*, pages 3192–3199, 2013.
- [30] Gunnar A Sigurdsson, Gül Varol, Xiaolong Wang, Ali Farhadi, Ivan Laptev, and Abhinav Gupta. Hollywood in homes: Crowdsourcing data collection for activity understanding. In *Proceedings of the European Conference on Computer Vision: 14th European Conference, Amsterdam, The Netherlands, October 11–14, 2016, Proceedings, Part I* 14, pages 510–526. Springer, 2016.
- [31] Hang Zhao, Antonio Torralba, Lorenzo Torresani, and Zhicheng Yan. Hacs: Human action clips and segments dataset for recognition and temporal localization. In *Proceedings of the IEEE International Conference on Computer Vision*, pages 8668–8678, 2019.
- [32] Christian Schudt, Ivan Laptev, and Barbara Caputo. Recognizing human actions: A local svm approach. In *Proceedings of the International Conference on Pattern Recognition*, volume 3, pages 32–36. IEEE, 2004.
- [33] Moshe Blank, Lena Gorelick, Eli Shechtman, Michal Irani, and Ronen Basri. Actions as space-time shapes. In *Proceedings of the IEEE International Conference on Computer Vision*, volume 2, pages 1395–1402. IEEE, 2005.
- [34] Karen Simonyan and Andrew Zisserman. Two-stream convolutional networks for action recognition in videos. *Advances in Neural Information Processing Systems*, 27, 2014.
- [35] Limin Wang, Yuanjun Xiong, Zhe Wang, Yu Qiao, Dahua Lin, Xiaoou Tang, and Luc Van Gool. Temporal segment networks for action recognition in videos. *IEEE Transactions on Pattern Analysis and Machine Intelligence*, 41(11):2740–2755, 2018.
- [36] Jeffrey Donahue, Lisa Anne Hendricks, Sergio Guadarrama, Marcus Rohrbach, Subhashini Venugopalan, Kate Saenko, and Trevor Darrell. Long-term recurrent convolutional networks for visual recognition and description. In *Proceedings of the IEEE Conference on Computer Vision and Pattern Recognition*, pages 2625–2634, 2015.
- [37] Christoph Feichtenhofer, Axel Pinz, and Andrew Zisserman. Convolutional two-stream network fusion for video action recognition. In *Proceedings of the IEEE Conference on Computer Vision and Pattern Recognition*, pages 1933–1941, 2016.
- [38] Bolei Zhou, Alex Andonian, Aude Oliva, and Antonio Torralba. Temporal relational reasoning in videos. In *Proceedings of the European Conference on Computer Vision*, pages 803–818, 2018.
- [39] Ji Lin, Chuang Gan, and Song Han. Tsm: Temporal shift module for efficient video understanding. In *Proceedings of the IEEE International Conference on Computer Vision*, pages 7083–7093, 2019.

- [40] Xiaolong Wang, Ross Girshick, Abhinav Gupta, and Kaiming He. Non-local neural networks. In *Proceedings of the IEEE Conference on Computer Vision and Pattern Recognition*, pages 7794–7803, 2018.
- [41] Du Tran, Heng Wang, Lorenzo Torresani, Jamie Ray, Yann LeCun, and Manohar Paluri. A closer look at spatiotemporal convolutions for action recognition. In *Proceedings of the IEEE Conference on Computer Vision and Pattern Recognition*, pages 6450–6459, 2018.
- [42] Ali Diba, Mohsen Fayyaz, Vivek Sharma, Amir Hossein Karami, Mohammad Mahdi Arzani, Rahman Yousefzadeh, and Luc Van Gool. Temporal 3d convnets: New architecture and transfer learning for video classification. *arXiv preprint arXiv:1711.08200*, 2017.
- [43] Navneet Dalal and Bill Triggs. Histograms of oriented gradients for human detection. In *Proceedings of the IEEE Conference on Computer Vision and Pattern Recognition*, volume 1, pages 886–893. Ieee, 2005.
- [44] Navneet Dalal, Bill Triggs, and Cordelia Schmid. Human detection using oriented histograms of flow and appearance. In *Proceedings of the European Conference on Computer Vision: 9th European Conference on Computer Vision*, Graz, Austria, May 7–13, 2006. *Proceedings, Part II* 9, pages 428–441. Springer, 2006.
- [45] Bingbing Ni, Xiaokang Yang, and Shenghua Gao. Progressively parsing interactional objects for fine grained action detection. In *Proceedings of the IEEE Conference on Computer Vision and Pattern Recognition*, pages 1020–1028, 2016.
- [46] Jonathan Munro and Dima Damen. Multi-modal domain adaptation for fine-grained action recognition. In *Proceedings of the IEEE Conference on Computer Vision and Pattern Recognition*, pages 122–132, 2020.
- [47] James Hong, Matthew Fisher, Michaël Gharbi, and Kayvon Fatahalian. Video pose distillation for few-shot, fine-grained sports action recognition. In *Proceedings of the IEEE International Conference on Computer Vision*, pages 9254–9263, 2021.
- [48] Fang Liu, Liang Zhao, Xiaochun Cheng, Qin Dai, Xiangbin Shi, and Jianzhong Qiao. Fine-grained action recognition by motion saliency and mid-level patches. *Applied Sciences*, 10(8):2811, 2020.
- [49] Lei Chen, Zhan Tong, Yibing Song, Gangshan Wu, and Limin Wang. Cycleacr: Cycle modeling of actor-context relations for video action detection. *arXiv preprint arXiv:2303.16118*, 2023.
- [50] Christoph Feichtenhofer. X3d: Expanding architectures for efficient video recognition. In *Proceedings of the IEEE Conference on Computer Vision and Pattern Recognition*, pages 203–213, 2020.
- [51] Jiajun Tang, Jin Xia, Xinzhi Mu, Bo Pang, and Cewu Lu. Asynchronous interaction aggregation for action detection. In *Proceedings of the European Conference on Computer Vision: 16th European Conference, Glasgow, UK, August 23–28, 2020, Proceedings, Part XV* 16, pages 71–87. Springer, 2020.
- [52] Junting Pan, Siyu Chen, Mike Zheng Shou, Yu Liu, Jing Shao, and Hongsheng Li. Actor-context-actor relation network for spatio-temporal action localization. In *Proceedings of the IEEE Conference on Computer Vision and Pattern Recognition*, pages 464–474, 2021.
- [53] Ashish Vaswani, Noam Shazeer, Niki Parmar, Jakob Uszkoreit, Llion Jones, Aidan N Gomez, Lukasz Kaiser, and Illia Polosukhin. Attention is all you need. *Advances in Neural Information Processing Systems*, 30, 2017.
- [54] Guang Li, Linchao Zhu, Ping Liu, and Yi Yang. Entangled transformer for image captioning. In *Proceedings of the IEEE International Conference on Computer Vision*, pages 8928–8937, 2019.
- [55] Limin Wang, Bingkun Huang, Zhiyu Zhao, Zhan Tong, Yinan He, Yi Wang, Yali Wang, and Yu Qiao. Videomae v2: Scaling video masked autoencoders with dual masking. In *Proceedings of the IEEE Conference on Computer Vision and Pattern Recognition*, pages 14549–14560, 2023.
- [56] Yufei Xu, Jing Zhang, Qiming Zhang, and Dacheng Tao. Vitpose: Simple vision transformer baselines for human pose estimation. *Advances in Neural Information Processing Systems*, 35:38571–38584, 2022.
- [57] Yufei Xu, Jing Zhang, Qiming Zhang, and Dacheng Tao. Vitpose++: Vision transformer for generic body pose estimation. *IEEE Transactions on Pattern Analysis and Machine Intelligence*, 46(2):1212–1230, 2024.
- [58] Rohit Girdhar, Joao Carreira, Carl Doersch, and Andrew Zisserman. Video action transformer network. In *Proceedings of the IEEE Conference on Computer Vision and Pattern Recognition*, pages 244–253, 2019.
- [59] Dingfeng Shi, Yujie Zhong, Qiong Cao, Jing Zhang, Lin Ma, Jia Li, and Dacheng Tao. React: Temporal action detection with relational queries. In *Proceedings of the European Conference on Computer Vision*, pages 105–121. Springer, 2022.
- [60] Lei Chen, Zhan Tong, Yibing Song, Gangshan Wu, and Limin Wang. Efficient video action detection with token dropout and context refinement. In *Proceedings of the IEEE International Conference on Computer Vision*, pages 10388–10399, 2023.
- [61] Shoufa Chen, Peize Sun, Enze Xie, Chongjian Ge, Jiannan Wu, Lan Ma, Jiajun Shen, and Ping Luo. Watch only once: An end-to-end video action detection framework. In *Proceedings of the IEEE International Conference on Computer Vision*, pages 8158–8167, 2021.
- [62] Jiaojiao Zhao, Yanyi Zhang, Xinyu Li, Hao Chen, Shuai Bing, Mingze Xu, Chunhui Liu, Kaustav Kundu, Yuanjun Xiong, Davide Modolo, et al. Tubenet: Tubelet transformer for video action detection. *arXiv preprint arXiv:2104.00969*, 2021.
- [63] Tao Wu, Mengqi Cao, Ziteng Gao, Gangshan Wu, and Limin Wang. Stmixer: A one-stage sparse action detector. In *Proceedings of the IEEE Conference on Computer Vision and Pattern Recognition*, pages 14720–14729, 2023.
- [64] Peize Sun, Rufeng Zhang, Yi Jiang, Tao Kong, Chenfeng Xu, Wei Zhan, Masayoshi Tomizuka, Lei Li, Zehuan Yuan, Changhu Wang, et al. Sparse r-cnn: End-to-end object detection with learnable proposals. In *Proceedings of the IEEE Conference on Computer Vision and Pattern Recognition*, pages 14454–14463, 2021.
- [65] Nicolas Carion, Francisco Massa, Gabriel Synnaeve, Nicolas Usunier, Alexander Kirillov, and Sergey Zagoruyko. End-to-end object detection with transformers. In *Proceedings of the European Conference on Computer Vision*, pages 213–229. Springer, 2020.
- [66] Chaitanya Ryali, Yuan-Ting Hu, Daniel Bolya, Chen Wei, Haoqi Fan, Po-Yao Huang, Vaibhav Aggarwal, Arkabandhu Chowdhury, Omid Poursaeed, Judy Hoffman, et al. Hiera: A hierarchical vision transformer without the bells-and-whistles. In *Proceedings of the International Conference on Machine Learning*, pages 29441–29454. PMLR, 2023.
- [67] MMAAction2 Contributors. Openmmlab's next generation video understanding toolbox and benchmark. <https://github.com/open-mmlab/mmdetection>, 2020.
- [68] Kai Chen, Jiaqi Wang, Jiangmiao Pang, Yuhang Cao, Yu Xiong, Xiaoxiao Li, Shuyang Sun, Wansen Feng, Ziwei Liu, Jiarui Xu, Zheng Zhang, Dazhi Cheng, Chenchen Zhu, Tianheng Cheng, Qijie Zhao, Buyu Li, Xin Lu, Rui Zhu, Yue Wu, Jifeng Dai, Jingdong Wang, Jianping Shi, Wanli Ouyang, Chen Change Loy, and Dahua Lin. MMDetection: Open mmlab detection toolbox and benchmark. *arXiv preprint arXiv:1906.07155*, 2019.
- [69] Tsung-Yi Lin, Michael Maire, Serge Belongie, James Hays, Pietro Perona, Deva Ramanan, Piotr Dollár, and C Lawrence Zitnick. Microsoft coco: Common objects in context. In *Proceedings of the European Conference on Computer Vision: 13th European Conference, Zurich, Switzerland, September 6–12, 2014, Proceedings, Part V* 13, pages 740–755. Springer, 2014.
- [70] Tsung-Yi Lin, Priya Goyal, Ross Girshick, Kaiming He, and Piotr Dollár. Focal loss for dense object detection. In *Proceedings of the IEEE International Conference on Computer Vision*, pages 2980–2988, 2017.
- [71] Shilong Liu, Feng Li, Hao Zhang, Xiao Yang, Xianbiao Qi, Hang Su, Jun Zhu, and Lei Zhang. Dab-detr: Dynamic anchor boxes are better queries for detr. 2022.
- [72] Shilong Zhang, Xinjiang Wang, Jiaqi Wang, Jiangmiao Pang, Chengqi Lyu, Wenwei Zhang, Ping Luo, and Kai Chen. Dense distinct query for end-to-end object detection. In *Proceedings of the IEEE Conference on Computer Vision and Pattern Recognition*, pages 7329–7338, 2023.
- [73] Jia Deng, Wei Dong, Richard Socher, Li-Jia Li, Kai Li, and Li Fei-Fei. Imagenet: A large-scale hierarchical image database. In *Proceedings of the IEEE Conference on Computer Vision and Pattern Recognition*, pages 248–255. IEEE, 2009.
- [74] Diederik P Kingma and Jimmy Ba. Adam: A method for stochastic optimization. In *Proceedings of the International Conference on Learning Representations*, 2015.
- [75] Alexander Kirillov, Eric Mintun, Nikhila Ravi, Hanzi Mao, Chloe Rolland, Laura Gustafson, Tete Xiao, Spencer Whitehead, Alexander C Berg, Wan-Yen Lo, et al. Segment anything. *arXiv preprint arXiv:2304.02643*, 2023.
- [76] Jun Liu, Amir Shahroudy, Mauricio Perez, Gang Wang, Ling-Yu Duan, and Alex C Kot. Ntu rgb+ d 120: A large-scale benchmark for 3d human activity understanding. *IEEE Transactions on Pattern Analysis and Machine Intelligence*, 42(10):2684–2701, 2019.
- [77] Amir Shahroudy, Jun Liu, Tian-Tsong Ng, and Gang Wang. Ntu rgb+ d: A large scale dataset for 3d human activity analysis. In *Proceedings of the IEEE Conference on Computer Vision and Pattern Recognition*, pages 1010–1019, 2016.
- [78] Sijie Yan, Yuanjun Xiong, and Dahua Lin. Spatial temporal graph convolutional networks for skeleton-based action recognition. In *Proceedings of the Association for the Advancement of Artificial Intelligence Conference*, volume 32, 2018.
- [79] Ilya Loshchilov and Frank Hutter. Decoupled weight decay regularization. In *Proceedings of the International Conference on Learning Representations*, 2019.

A Appendix

A.1 FHA-Kitchens Dataset

A.1.1 Data Annotation.

We recruited 10 voluntary annotators to annotate hand actions for each frame with high quality. Their responsibility was to annotate bounding boxes and multi-granularity action categories for each hand interaction region. To enhance annotation efficiency, we implemented a parallel annotation approach. We utilized the LabelBee tool for annotating bounding boxes and coarse-grained categories, while fine-grained action triplets were annotated on the Amazon Mechanical Turk platform. To ensure annotation quality, we conducted three rounds of cross-checking and corrections. In the main paper, we described the annotation details for bounding boxes and categories. In addition to this, we also provide segment annotations for the objects.

Bounding Box Annotation. During annotation, we may encounter overlapping bounding boxes, *i.e.*, the same interacting object will satisfy two annotation definitions, for example, the *utility knife* in Figure 6, which is both the object directly touched by the right hand in the R-O interaction region and the active force provider in the O-O interaction region. In this case, we annotated all the labels because the same object participates in different interaction actions and has different roles (The corresponding visualizations are shown in Figure 6 and the annotation details are listed in Figure 7). Finally, we annotated a total of 198,839 bounding boxes over 9 types, including 49,746 hand boxes, 66,402 interaction region boxes, and 82,691 interaction object boxes. Compared to existing datasets [4], we added an average of 5 additional annotation types per frame.

Object Segment Annotation. To enrich our FHA-Kitchens, we utilized the state-of-the-art SAM model [75] to annotate object masks in all video frames, which can be used for action segmentation relevant tasks.

A.1.2 More statistics of the FHA-Kitchens Dataset.

In this part, we re-arrange some figures in the paper to make them more readable and provide more statistics of the FHA-Kitchens dataset. Our annotation primarily focuses on hand interaction regions, interaction objects, and their corresponding interaction actions, resulting in a diverse array of verbs, nouns, and bounding boxes.

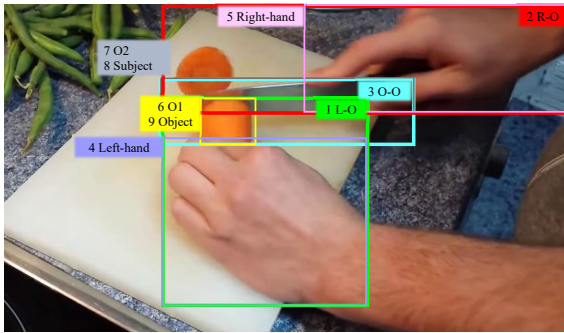


Figure 6: Visualization of bounding box annotations for the example of “fry vegetables”.

Verbs. The annotated dataset comprises 130 action verbs that have been grouped into 43 parent verb categories (Figure 8 and Figure 9). The three most prevalent parent verb categories, based on the count of sub-action verbs, are *Cut*, *Hold*, and *Take*, representing the most frequently occurring hand actions in human interactions. Figure 9 visually depicts the distribution of all verb categories within FHA-Kitchens, ensuring the presence of at least one instance for each verb category. Specifically, the mapping between action verb IDs and their corresponding category names can be seen in Table 16.

Nouns. In our annotation process, we identified a total of 384 interaction object noun categories that are associated with actions, categorized into 17 super-categories. Figure 18 shows the distribution of noun categories based on their affiliations with super-categories. Notably, the super-category “vegetables & plants” exhibits the highest number of sub-categories, followed by “kitchenware”, which aligns with typical kitchen scenes. Specifically, the mapping between interaction object noun IDs and their corresponding category names can be seen in Table 17, Table 18, and Table 19.

Bounding Boxes. We performed a comprehensive statistical analysis on the bounding boxes of the three hand interaction regions and the corresponding interacting objects. Specifically, we focused on two aspects: the box area and the aspect ratio. Detailed results can be found in Figure 10 and Figure 11. Figure 10 shows the considerable range of sizes covered by our bounding boxes, with many interaction objects exhibiting small and challenging sizes for accurate detection. Moreover, in Figure 11, the aspect ratios of the bounding boxes exhibit notable variation. The aspect ratios of the three regions tend to concentrate within the range of [0.5,2], which can be attributed to the typical composition of interaction regions involving two interacting objects. Consequently, the bounding box encompasses the combined region of both objects. For instance, the R-O interaction region frequently involves the interaction between the “right hand” and “utility knife”. In such cases, the aspect ratio of the bounding box is observed to be 2:1, as depicted in Figure 6. These findings highlight the significant challenges of the detection task in our dataset.

Long-tail Property. The distribution of instances per action triplet category in FHA-Kitchens, as depicted in Figure 12, depicts a long-tail property. This distribution reflects the frequency of hand interactions in real-world kitchen scenes, taking into account the varying commonness or rarity of specific hand actions. For instance,

Bounding Box Annotation		Action Triplets Annotation	
<i>id</i>	<i>definition</i>	<i>b-box label</i>	<i>action triplet label</i>
1	left hand-object interaction region	L-O	(hand_left, press-on, carrot_end)
2	right hand-object interaction region	R-O	(hand_right, hold-in, utility-knife_handle)
3	object-object interaction region	O-O	(utility-knife_body, cut-slice, carrot_head)
4	left hand	Left-hand	-
5	right hand	Right-hand	-
6	object touched by left hand in L-O	O1	-
7	object touched by right hand in R-O	O2	-
8	active force provider in O-O	Subject	-
9	passive force receiver in O-O	Object	-

Figure 7: Descriptive list of action triplets and bounding box annotations.

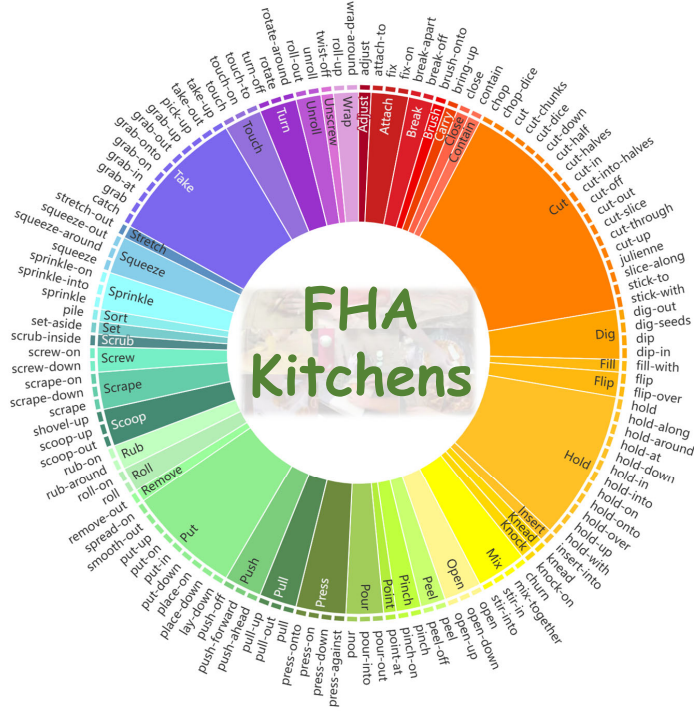


Figure 8: An overview of the action verbs and their parent action categories in FHA-Kitchens.

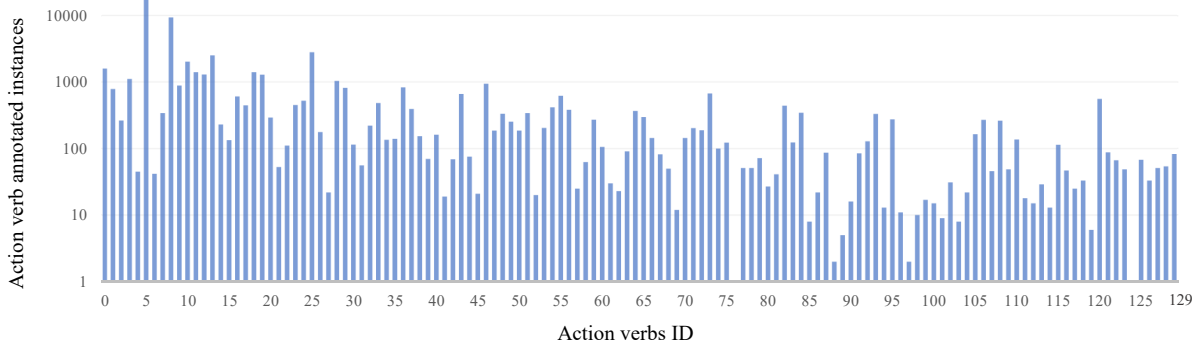


Figure 9: The distribution of instances per action verb category (the outer ring of the circle in Figure 8) in the FHA-Kitchens dataset.

the action triplet “<hand_right, hold-in, utility-knife_handle>” consists of 9,887 instances, which is nine times more prevalent than the “<hand_left, hold-in, utility-knife_handle>” triplet. This long-tail characteristic of the distribution renders FHA-Kitchens a challenging benchmark for hand action recognition, making it suitable for investigating few-shot learning and out-of-distribution generalization in action recognition as well.

A.1.3 More quantitative and qualitative results.

1) Quantitative Results

SL-AR Track: Supervised Learning for Fine-grained Hand Action Recognition

Settings. The SL-AR track primarily evaluates the performance of different action recognition models on fine-grained hand actions.

We adopted the representative TSN [11] and Slowfast [12] with the ResNet50 and ResNet101 backbones, VideoSwin [13] with the Swin-B backbone, VideoMAE V2 [55] with the three different size backbones, and HierA [66] with the HierA-B backbone. We trained these models on the FHA-Kitchens dataset using two settings: (1) **Pre-training on Kinetics 400 [10] and hybrid dataset**, where we initialized the backbone with Kinetics 400 or Hybrid dataset pre-trained weights and fine-tuned the entire model on the FHA-Kitchens training set; and (2) **Training from scratch on FHA-Kitchens**, where we randomly initialized the model weights and directly train them on FHA-Kitchens. For different models, we used

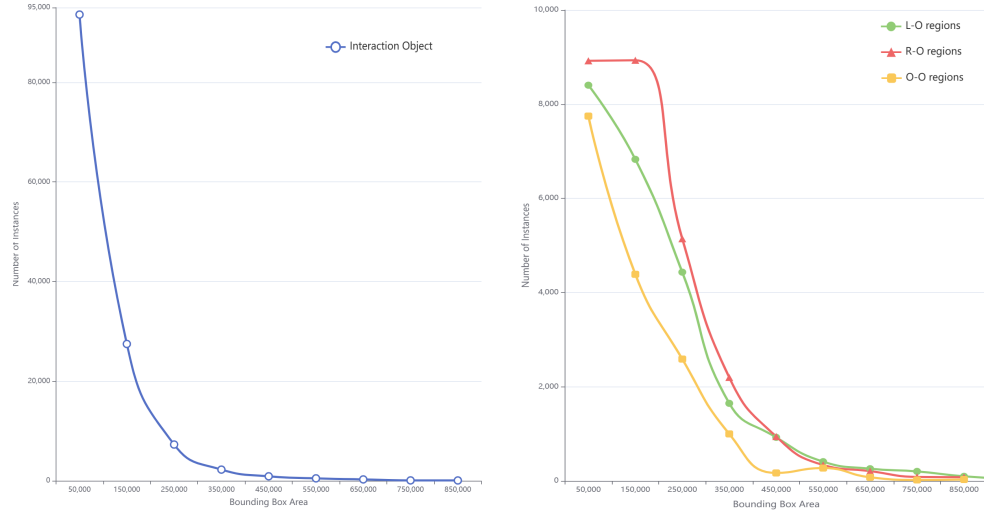


Figure 10: The distributions of bounding box areas of interaction objects (left) and interaction regions (right) in the FHA-Kitchens dataset.

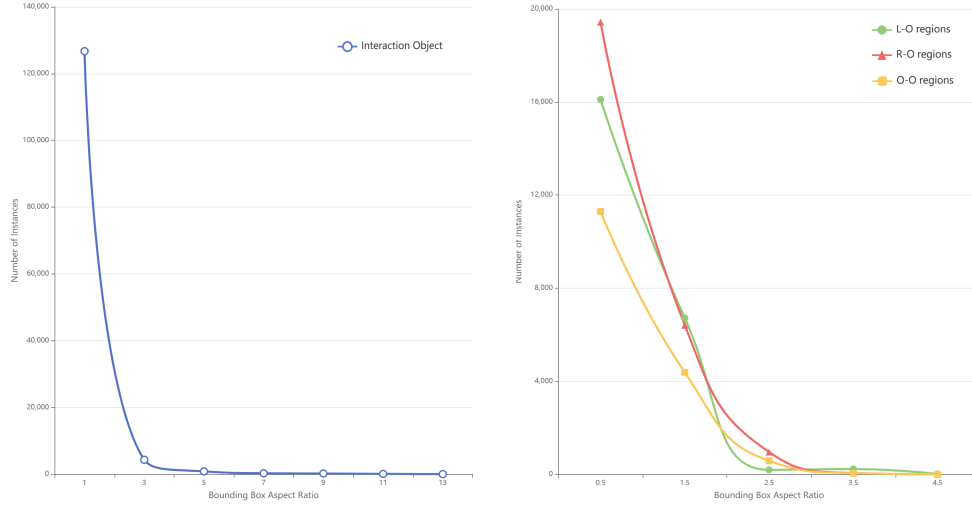


Figure 11: The distributions of bounding box aspect ratios of interaction objects (left) and interaction regions (right) in the FHA-Kitchens dataset.

the recommended optimization strategy and batch size, and the maximum training period was set to 210 epochs.

Results on the SL-AR Track. Table 6 presents the performance of different action recognition methods on the Kinetics 400 [10] dataset and the proposed FHA-Kitchens dataset, with and without pre-trained models. From the experimental results, it can be observed that the performance trends of all action recognition methods on FHA-Kitchens are similar to their performance on Kinetics 400 [10], while the models perform much better on the coarse-grained actions of Kinetics 400. For the best-performing VideoSwin [13] model, the top-1 accuracy on Kinetics 400 surpasses

the top-1 accuracy on FHA-Kitchens by 43.44%. And those methods with even large models cannot achieve satisfactory performance. This is clear evidence that validates the challenging nature of the fine-grained hand action recognition on FHA-Kitchens. Besides, the utilization of pre-trained weights has proven to be beneficial, resulting in improved accuracy compared to training models from scratch. This finding suggests that despite the existence of a domain gap between coarse-grained and fine-grained actions, pre-training remains an effective strategy for addressing the challenges inherent in FHA-Kitchens, which have a larger number of action categories and relatively limited training data.

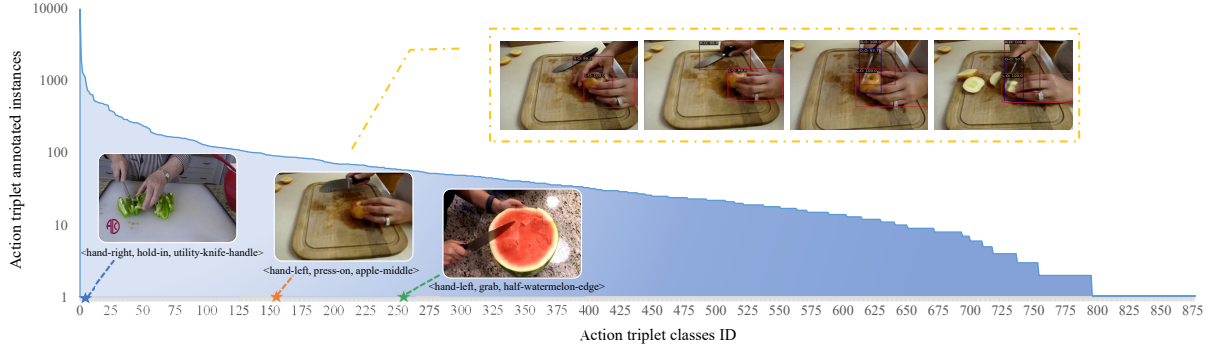


Figure 12: The distribution of instances per action triplet category in the FHA-Kitchens dataset.

Table 6: Classification results (Top-1 and Top-5 accuracy) of fine-grained hand actions using different methods on the validation set of the SL-AR track. w/ Pre-train : using pre-trained weights. w/o Pre-train: Training from scratch (the Kinetics 400 [10] dataset results from mmaction2 [67], VideoMAE V2 [55], and Hiera [66]).

Dataset	Method	Backbone	Pre-train Data	w/ Pre-train		w/o Pre-train	
				Top-1	Top-5	Top-1	Top-5
Kinetics 400	TSN [11]	ResNet50	ImageNet	72.83	90.65	-	-
		ResNet101	ImageNet	75.89	92.07	-	-
	SlowFast [12]	ResNet50	-	-	-	76.65	92.86
		ResNet101	-	-	-	78.65	93.88
	VideoSwin [13]	Swin-B	ImageNet	80.57	94.49	-	-
	VideoMAE V2 [55]	ViT-B	UnlabeledHybrid	81.50	-	-	-
		ViT-L	UnlabeledHybrid	85.40	-	-	-
		ViT-H	UnlabeledHybrid	86.90	-	-	-
	Hiera [66]	Hiera-B	Kinetics 400	84.00	-	-	-
Dataset	Method	Backbone	Pre-train Data	w/ Pre-train		w/o Pre-train	
				Top-1	Top-5	Top-1	Top-5
FHA-Kitchens	TSN [11]	ResNet50	Kinetics 400	30.37	74.26	29.11	73.84
		ResNet101	Kinetics 400	30.80	73.42	30.38	74.26
	SlowFast [12]	ResNet50	Kinetics 400	33.33	70.46	27.85	68.35
		ResNet101	Kinetics 400	36.71	67.93	31.22	69.62
	VideoSwin [13]	Swin-B	Kinetics 400	37.13	70.89	34.18	66.67
	VideoMAE V2 [55]	ViT-B	UnlabeledHybrid	21.67	57.08	-	-
		ViT-L	UnlabeledHybrid	32.92	68.75	-	-
		ViT-H	UnlabeledHybrid	34.58	68.33	-	-
	Hiera [66]	Hiera-B	Kinetics 400	27.00	69.20	-	-

In addition, we further supplemented the hand pose information and conducted experiments using the skeleton-based STGCN [78] method. We used STGCN pre-trained on NTU60 [77] and NTU120 [76] and fine-tuned the models on the SL-AR track using different features for fine-grained hand actions, the results (Top-1 and Top-5 accuracy) can be seen in Table 7.

According to the experimental results, it can be observed that 3D pose features outperform 2D pose features and bone features achieve better results than joint features. Nevertheless, the overall results did not surpass the efficacy of hand-object interaction-based approaches, highlighting that relying only on hand pose

information is insufficient for accomplishing fine-grained action recognition tasks. Because the generation of hand actions involves interacting objects, achieving a fine-grained hand action recognition task is required to consider the information of the objects interacting with the hand, which is different from a whole-body action recognition task (e.g., AVA, FineGym dataset).

DG Track: Intra- and Inter-class Domain Generalization for Interaction Region Detection

• Intra-class Domain Generalization

Settings. We conducted intra-class DG experiments using the three most prevalent parent action categories, i.e., *Cut*, *Hold*, and

Table 7: Classification results (Top-1 and Top-5 accuracy) of fine-grained hand actions using different features and the skeleton-based STGCN [78] method (pre-trained on NTU60 [77] and NTU120 [76]) on the validation set of the SL-AR track.

Pre-train Data	Feature	Top-1	Top-5	Pre-train Data	Feature	Top-1	Top-5
NTU60	joint-2d	22.78	47.68	NTU120	joint-2d	20.68	48.10
	joint-3d	22.36	52.32		joint-3d	21.10	47.68
	joint-motion-2d	8.02	19.83		joint-motion-2d	9.28	20.25
	joint-motion-3d	10.97	23.63		joint-motion-3d	11.81	26.16
	bone-2d	22.36	49.79		bone-2d	24.05	57.81
	bone-3d	24.05	52.32		bone-3d	24.05	51.05
	bone-motion-2d	10.55	23.21		bone-motion-2d	9.28	23.21
	bone-motion-3d	13.50	26.16		bone-motion-3d	12.24	27.00

Table 8: Intra-class DG test results of Faster RCNN [14] with the ResNet50 backbone on the “Cut” Setting. $\Delta_i = \frac{1}{3} \sum_{j,j \neq i} ji - ii$, $\Delta_i^* = \frac{1}{3} \sum_{j,j \neq i} ij - ii$, $i = 0, 1, 2, 3$.

Train	Test (mAP)				Δ^*
	cut-slice	cut-off	cut-down	cut-dice	
w/o cut-slice	33.30	65.00	56.00	60.90	27.33
w/o cut-off	57.10	48.00	54.80	62.80	10.23
w/o cut-down	57.30	64.40	41.30	63.50	20.43
w/o cut-dice	57.50	64.90	58.70	41.10	19.27
Δ	24.00	16.77	15.20	21.30	

Table 9: Intra-class DG test results of Faster RCNN [14] with the ResNet50 backbone on the “Hold” Setting. $\Delta_i = \frac{1}{2} \sum_{j,j \neq i} ji - ii$, $\Delta_i^* = \frac{1}{2} \sum_{j,j \neq i} ij - ii$, $i = 0, 1, 2$.

Train	Test (mAP)			Δ^*
	hold-up	hold-in	hold-around	
w/o hold-up	44.00	53.50	71.70	18.60
w/o hold-in	44.30	7.30	69.10	49.40
w/o hold-around	52.30	52.80	47.80	4.75
Δ	4.30	45.85	22.60	

Table 10: Intra-class DG test results of Faster RCNN [14] with the ResNet50 backbone on the “Take” Setting. $\Delta_i = \frac{1}{2} \sum_{j,j \neq i} ji - ii$, $\Delta_i^* = \frac{1}{2} \sum_{j,j \neq i} ij - ii$, $i = 0, 1, 2$.

Train	Test (mAP)			Δ^*
	pick-up	grab	catch	
w/o pick-up	0.40	47.10	46.60	46.45
w/o grab	19.00	4.50	39.00	24.50
w/o catch	19.10	46.00	15.60	16.95
Δ	18.65	42.05	27.20	

Take. For each parent action category, we selected the most prevalent sub-categories and adopted the cross-validation protocol,

i.e., randomly choosing one sub-category as the test set while using all other sub-categories for training. Following the SL-AD track, we selected the Faster RCNN [14] model with the ResNet50 backbone as the default model, which is pre-trained on the MS COCO [69] object detection dataset.

Results on the Intra-class DG Track. The results on *Cut*, *Hold*, and *Take* are summarized in Table 8, 9, and 10. In the “*Cut*” parent category, the performance of all four detection models remains stable for the sub-categories seen during training but deteriorates for unseen sub-categories, as evidenced by the diagonal scores, which exhibit a minimum drop of 15 mAP. The findings in the results of the other two parent categories align with the observations in the “*Cut*” parent category. This finding suggests that there is still potential for enhancing the models’ generalization abilities, e.g., by exploring the domain generalization or unsupervised domain adaptation techniques.

• Inter-class Domain Generalization

Settings. We chose the three most prevalent parent action categories *Cut*, *Hold*, and *Take*, and adopted the cross-validation protocol, i.e., randomly choosing one parent category for training and using the other parent categories for testing. Other settings follow those in the intra-class DG track.

Results on the Inter-class DG Track. The results are listed in Table 11. Similar to the results in the intra-class DG track, the detection models perform well on the seen categories while deteriorating on the unseen categories. Nevertheless, it is interesting to find that the performance gap ($\Delta_0 = 6.05$ and $\Delta_0^* = 8.05$) between *Cut* and others are smaller than those in the intra-class DG track, implying that there is likely a large intra-class variance,

Table 11: Inter-class DG test results. $\Delta_i = ii - \frac{1}{2} \sum_{j,j \neq i} ji$, $\Delta_i^* = ii - \frac{1}{2} \sum_{j,j \neq i} ij$, $i = 0, 1, 2$.

Train	Test (mAP)			Δ^*
	Cut	Hold	Take	
Cut	37.40	29.50	29.20	8.05
Hold	48.70	52.30	41.80	7.05
Take	14.00	13.20	41.20	27.60
Δ	6.05	30.95	5.70	

Table 12: Comparative experiments of the action dimensional weight, i.e., hyper-parameter w_d ($d \in \{s, a, o\}$), under different ratio settings. $w_s = w_o = (1 - w_a)/2$, $w_s + w_a + w_o = 1$, **M-G: Mixed-Grained.**

Method	Backbone	Train Data	w_a	M-G mAP(%)
Ours-4scale	ResNet-50	Multi-Granularity	0.5	54.9
			0.6	57.0
			0.7	55.6
			0.8	56.0
			0.9	54.7
Ours-5scale	Swin-L	Multi-Granularity	0.5	57.2
			0.6	59.4
			0.7	58.2
			0.8	57.4
			0.9	57.1

and the detection model is prone to overfitting the seen categories, particularly when the volume of training data is smaller (there are 7,463 training frames in *Hold* while only 1,680 in *Take*).

2) Qualitative Results

The visual results of the SL-AD and SL-AR track experiments are presented in Figure 15, Figure 16, and Figure 17. We showcased the visualization results of interaction region detection, interacting object detection, and action recognition, focusing on hand interaction scenarios of varying complexity. In the interaction region detection results, we provide coarse-grained action categories corresponding to the sub-interaction regions, i.e., $\langle L-O, R-O, O-O \rangle$. In the recognition results, we provide fine-grained action verbs corresponding to the three hand sub-interaction regions, denoted as $\langle L-O \text{ action verb}, R-O \text{ action verb}, O-O \text{ action verb} \rangle$. Figure 15 shows some challenging cases of hand interactions, providing compelling evidence of the good prediction performance of detection and recognition models, i.e., the Faster-RCNN [14] with a ResNet50 backbone for detection and a pre-trained TSN [11] model with a ResNet50 backbone for action recognition. Moreover, Figure 16 and Figure 17 also demonstrate accurate detection and recognition results for some common interaction cases.

A.2 MG-HAD: Multi-Granularity Hand Action Detection

A.2.1 Multi-dimensional Action Queries.

To enhance the model’s understanding of multi-dimensional action information from global and local perspectives, in our design of multi-dimensional action queries, we introduce an action dimensional hyper-parameter w_d ($d \in \{s, a, o\}$), to control the proportion of local information (sub-categories) fused with global information (triplet categories). In the three action dimensions $\langle s, a, o \rangle$, the a dimension is the most crucial for our task. Therefore, we use w_a as the key weight to dynamically adjust the weight proportions of the three action dimensions, with a total sum of 1. To determine the optimal weight distribution, we conducted a total of 10 comparative experiments under different backbones, with detailed results

provided in Table 12. Based on the experimental results, the action dimensional weight setting we selected is as follows:

$$w_d = \begin{cases} 0.6 & \text{if } d = a \\ 0.2 & \text{if } d = s \text{ or } d = o \end{cases}, \quad (4)$$

where $w_s = w_o = (1 - w_a)/2$, $w_s + w_a + w_o = 1$.

A.2.2 Coarse-Fine Contrastive DeNoising (C-F CDN).

To enable the model to handle multi-granularity hand action labels and understand the differences between different granularity labels, we propose the C-F CDN module. When designing the noise label generation strategy, we replaced the “random” generation of noise with “specified”, reducing randomness by specifying noise positions and categories. This ensures noise is added to different granularity labels, generating CDN queries encompassing various granularity. To determine the optimal setting, we considered the noise distribution of different granularity categories in real-world scenarios and ensured contrastive learning between coarse- and fine-grained information. We conducted three sets of comparative experiments (see Table 13). The final selected setting, as shown in Eq. (5), exhibits the most significant improvement. Hence, subsequent experiments were conducted using this setting for further investigation. Our method’s success lies in its ability to suppress confusion at the category level and select appropriate granularity to predict hand action categories, thus enhancing its ability to predict multi-granularity information.

$$\text{noise label} = \begin{cases} \text{fine-grained} & i \in [0, 3) \\ \text{mixed-grained} & i \in [3, C) \end{cases}, \quad (5)$$

where i indexes the multi-granularity action category for a specific instance (i.e., 0~2 denote coarse-grained categories while 3~C-1 denote fine-grained categories), and C is the number of categories. “fine-grained” and “mixed-grained” denote that the noise label is chosen randomly from the fine-grained categories and the combination of the coarse-grained and fine-grained categories, respectively.

A.2.3 Action Detection Results of MG-HAD.

Visualization detection results. Based on the 5scale-Swin-L backbone, qualitative comparison results with the baseline [17] on the FHA-Kitchens dataset are shown in Figure 13. Our model accurately detects three hand sub-interaction regions (i.e., “Left hand-Object interaction region (L-O)”, “Right hand-Object interaction region (R-O)”, and “Object-Object interaction region (O-O)”) and provides multi-granularity hand action categories (i.e., “Coarse-Grained” and “Fine-Grained”). Compared to the DINO, we demonstrate superior performance across multiple dimensions of fine-grained categories, illustrating the effectiveness of our designed multi-dimensional action queries. Additionally, we present our model’s multi-granularity hand action detection results in more kitchen scenarios, as shown in Figure 14. We randomly selected four different kitchen scenarios, i.e., “fry vegetables”, “sandwich”, “salad”, and “fruit”, showcasing complex hand actions. Our model offers accurate bounding boxes and multi-granularity hand action information for three hand sub-interaction regions.

Basic Hyper-parameters. For the basic hyper-parameters, consistent with DINO [17], we utilized a 6-layer Transformer encoder and a 6-layer Transformer decoder with a hidden feature dimension of 256. We set the initial learning rate (lr) to 1×10^{-4} and employed a MultiStep lr scheduler, dropping lr by multiplying 0.1

Table 13: Three sets comparative experiments of the “noise label generation strategy” in the Coarse-Fine Contrastive DeNoising (C-F CDN). M-G: Mixed-Grained, C-G: Coarse-Grained, F-G: Fine-Grained.

Method	Backbone	Train Data	noisy label location	noisy label class	FHA-Kitchens val mAP(%)		
					M-G label	C-G sub-label	F-G sub-label
<i>Baseline</i> [17]	ResNet-50	multi-granularity	random	random	54.7	76.3	54.5
<i>Ours-4scale</i>			a_1 : fine-grained a_2 : coarse-grained	$a_1 \rightarrow$ mixed-grained $a_2 \rightarrow$ fine-grained	56.6	75.9	56.4
				$a_1 \rightarrow$ coarse-grained $a_2 \rightarrow$ fine-grained	56.1	75.5	55.8
				$a_1 \rightarrow$ coarse-grained $a_2 \rightarrow$ mixed-grained	55.8	74.5	55.6

at the 11-th and 20-th epochs for ResNet50, corresponding to the 12 and 24 epoch settings. We employed the AdamW [74, 79] optimizer with a weight decay of 1×10^{-4} and trained our model on NVIDIA GeForce RTX 3090 GPUs. The ResNet50 backbone was trained with a batch size of 2 per GPU, while the SwinL backbone had a batch size of 1. We initialized 900 decoder queries, maintaining the same computational cost as DINO. We provide detailed hyper-parameters in Table 15 for reproducibility.

A.3 Datasheets for Datasets

A.3.1 Motivation.

1. For what purpose was the dataset created? Was there a specific task in mind? Was there a specific gap that needed to be filled? Please provide a description.

A1: FHA-Kitchens is created to facilitate research in the field of complex multi-granularity hand action. It is important to study several challenging questions in the context of more training data from diverse multi-granularity hand actions, such as: (1) How do different representative action recognition models perform on fine-grained hand action tasks? (2) How do state-of-the-art detection models perform on the refined hand interaction regions with multi-granularity hand action categories? (3) How about the impact of pre-training, e.g., on the whole-body actions dataset [10], in the context of the large-scale dataset with diverse multi-granularity hand actions? and (4) How do the intra-class and inter-class generalization capabilities of models trained with specific fine-grained hand actions or parent hand actions perform? However, existing action datasets primarily focus on whole-body actions or coarse-grained action categories, lacking finer-grained hand-action localization and category information. Therefore, it is impossible to study these questions using existing datasets. In contrast, FHA-Kitchens primarily focuses on hand actions and refines hand interaction regions into three sub-interaction regions. We annotated coarse- and fine-grained actions for each sub-interaction region. Coarse-grained categories, denoted by the generic terms “L-O”, “R-O”, and “O-O”, represent the coarse actions within the sub-interaction regions. Fine-grained action category in a triplet format: $\langle \text{subject}, \text{action verb}, \text{object} \rangle$. Overall, we meticulously annotated 880 hand action categories (coarse- and fine-grained) for approximately 220k bounding boxes, with each category corresponding to a sub-interaction region’s localization box. Fine-grained categories per frame have

nine dimensions, resulting in 877 action triplets, significantly enhancing the granularity of actions and providing valuable resources for researchers to study these questions effectively.

FHA-Kitchens aims to provide a better, more comprehensive, and finer-grained benchmark for hand action. However, existing hand-action datasets exhibit limitations including insufficient representation of hand-action granularity, lack of annotation of hand-action interaction regions, and neglect of the relationships between interacting objects. With its diverse and finer-grained hand action information, the FHA-Kitchens dataset enables a better evaluation performance for hand action tasks.

2. Who created this dataset (e.g., which team, research group) and on behalf of which entity (e.g., company, institution, organization)?

A2: Our dataset is created by the authors as well as some volunteer undergraduate students from Wuhan University, including Ting Zhe, Yongqian Li, Chengli Chen, Xin Ding, Jiali Li, Tengzheng Li, RunFu Guo, Heng Gao, Xing Zhao, Weisheng Chen, Chaoyu Mai, Yipan Wei.

3. Who funded the creation of the dataset? If there is an associated grant, please provide the name of the grantor and the grant name and number.

A3: This work was supported in part by the National Key Research and Development Program of China under No. 2021YFC33002 00, the National Natural Science Foundation of China (Grant No. 62276195), and the Special Fund of Hubei LuoJia Laboratory under Grant 220100014.

A.3.2 Composition.

1. What do the instances that comprise the dataset represent (e.g., documents, photos, people, countries)? Are there multiple types of instances(e.g., movies, users, and ratings; people and interactions between them; nodes and edges)? Please provide a description.

A1: FHA-Kitchens consists of video clips, each video clip consists of consecutive video frames, including 880 coarse- and fine-grained hand action categories. For each frame, we provide bounding boxes for three hand sub-interaction regions (*i.e.*, left hand-object (L-O), right hand-object (R-O), and object-object (O-O) interaction regions) and the interaction objects. Each sub-interaction region action was annotated using coarse- and fine-grained action categories. Coarse-grained categories, denoted by the generic terms “L-O”, “R-O”, and “O-O”, fine-grained action category in a triplet format: $\langle \text{subject},$

action verb, object>. Additionally, we provide segmentation masks related to hands and interaction objects.

2. How many instances are there in total (of each type, if appropriate)?

A2: The FHA-Kitchens contains 30,047 frames from 2,377 video clips, with each frame annotated for three hand sub-interaction regions, resulting in a total of 877 fine-grained action triplets and 3 coarse-grained action categories. Among them, there are 597 frames where no hand interaction action occurs, represented as L-O_triplet:<none>, R-O_triplet:<none>, O-O_triplet:<none>.

3. Does the dataset contain all possible instances or is it a sample (not necessarily random) of instances from a larger set? If the dataset is a sample, then what is the larger set? Is the sample representative of the larger set (e.g., geographic coverage)? If so, please describe how this representativeness was validated/verified. If it is not representative of the larger set, please describe why not (e.g., to cover a more diverse range of instances, because instances were withheld or unavailable).

A3: FHA-Kitchens is a real-world sample of human hands part in the kitchen scenes, including information about their hand actions. The data is sourced from an existing large-scale whole-body action dataset [2], from which we selected videos featuring hand interaction actions. We extracted a total of 2,377 video clips, amounting to 84.22 minutes of footage, encompassing 8 distinct types of dishes. Due to the diversity of real-world human hand actions, it's impossible to cover all types of actions. The FHA-Kitchens dataset focuses primarily on multi-granularity hand action tasks. To address the granularity issue, we improved the hand action information in the existing dataset. Compared to the data's original annotations in Kinetics-700_2020 [2], our dataset expanded the action labels by 7 dimensions, increased the number of action categories by 52 times, and introduced 122 new action verbs. We provide a finer-grained set of hand-action instances than ever before, facilitating further research in hand-action.

4. What data does each instance consist of? "Raw" data (e.g., unprocessed text or images) or features? In either case, please provide a description.

A4: Each video frame consists of at most 9 types of bonding boxes (*i.e.*, three hand sub-interaction regions and interaction objects within interaction region) and sub-interaction region corresponding coarse- and fine-grained descriptions (*i.e.*, L-O, R-O, O-O, and <subject, action verb, object>). Additionally, we took into account the "active-passive" relationships between object pairs and the specific contact areas involved in the interaction actions. Consequently, our annotation process encompassed a total of nine dimensions, resulting in a total of 877 fine-grained hand action triplets and 3 coarse-grained hand action categories. The annotated visualizations are shown in Figure 6 and corresponding details are listed in Figure 7.

5. Is there a label or target associated with each instance? If so, please provide a description.

A5: Yes. Due to our parallel annotation process, we generated annotation files in different styles. However, we consolidated all the bounding box and triplet annotation information into a single CSV file. In the merged CSV file, each instance is annotated with labels following the style of the Kinetics [2, 10, 19, 20] and AVA [21] datasets, which include video_name, video_id, clip_id, clip_name,

frame_name, timestamp, L-O_triplet, L-O_action_verb_id, L-O_action_verb_class, L-O_action_bbox, left_hand_bbox, O1_class, O1_bbox, R-O_triplet, R-O_action_verb_id, R-O_action_verb_class, R-O_action_bbox, right_hand_bbox, O2_class, O2_bbox, O-O_triplet, O-O_action_verb_id, O-O_action_verb_class, O-O_action_bbox, subject_class, subject_bbox, object_class, object_bbox, action_verb_triplet, action_verb_triplet_id.

6. Is any information missing from individual instances? If so, please provide a description, explaining why this information is missing (e.g., because it was unavailable). This does not include intentionally removed information but might include, e.g., redacted text.

A6: Yes. Some instances may not have all 9 types of bonding boxes and their corresponding coarse-fine-grained action categories and segmentation annotation because of interaction action scenes, severe occlusion, truncation, blur, or small scale. We just annotated "None" in our annotation file to represent this situation.

7. Are relationships between individual instances made explicit (e.g., users' movie ratings, and social network links)? If so, please describe how these relationships are made explicit.

A7: Yes. We provide different styles of annotation files, in COCO-style, the annotations are connected by image id and category id, you can easily access them by COCO APIs. In CSV style, one line represents the annotations of one frame and can be processed by the pandas library easily.

8. Are there recommended data splits (e.g., training, development/validation, testing)? If so, please provide a description of these splits, explaining the rationale behind them.

A8: Yes. We randomly split the dataset into the disjoint train, validation, and test sets following the ratio of 7:1:2.

9. Are there any errors, sources of noise, or redundancies in the dataset? If so, please provide a description.

A9: Although we conducted three rounds of cross-checking and corrections, there may still be some errors in the annotations, *e.g.*, inappropriate bounding box annotations, or small drifts of the bounding box locations, incorrectly written verbs or nouns, insufficient granularity in verb or noun descriptions, inappropriate formatting of triplets, etc. However, we have made every effort to minimize such occurrences.

To analyze the quality of annotations, we randomly selected 500 frames and conducted manual evaluations for correctness. The results are reported in Table 14. These error rates are comparable to recently published datasets [4].

Table 14: Error rate in FHA-Kitchens. I-O: Interaction Objects, I-R: Interaction Regions.

	Frames	I-O Boxes	I-R Boxes	Verb	Noun
Total Number	500	3,006	1,503	1,503	2,006
Error Rate (%)	-	4.9	2.5	2.2	5.3

10. Is the dataset self-contained, or does it link to or otherwise rely on external resources (e.g., websites, tweets, other datasets)? If it links to or relies on external resources, a) are there guarantees that they will exist, and remain constant,

over time; b) are there official archival versions of the complete dataset (i.g., including the external resources as they existed at the time the dataset was created); c) are there any restrictions (e.g., licenses, fees) associated with any of the external resources that might apply to a future user? Please provide descriptions of all external resources and any restrictions associated with them, as well as links or other access points, as appropriate.

A10: Our dataset was derived from a large-scale publicly available dataset, namely Kinetics-700_2020 [2], which is publicly available for download from their website. The Kinetics dataset follows the Creative Commons Attribution 4.0 International License. We would like to express our gratitude to the authors for their significant contributions to the research community.

11. Does the dataset contain data that might be considered confidential (e.g., data that is protected by legal privilege or by doctor-patient confidentiality, data that includes the content of individuals' non-public communications)? If so, please provide a description.

A11: No.

12. Does the dataset contain data that, if viewed directly, might be offensive, insulting, threatening, or might otherwise cause anxiety? If so, please describe why.

A12: No.

A.3.3 Collection Process.

1. How was the data associated with each instance acquired? Was the data directly observable (e.g., raw text, movie ratings), reported by subjects (e.g., survey responses), or indirectly inferred/derived from other data (e.g., part-of-speech tags, model-based guesses for age or language)? If data was reported by subjects or indirectly inferred/derived from other data, was the data validated/verified? If so, please describe how.

A1: Our data was obtained from the existing large-scale publicly available dataset, namely Kinetics-700_2020 [2], which is publicly available for download from their website, and then further cleaned, frame segmented, and reorganized to obtain 2377 video clips. The annotation of fine-grained action triplets was carried out on the Amazon Mechanical Turk platform, while the bounding box and coarse-grained actions annotation was facilitated using the Label-Bee tool.

2. What mechanisms or procedures were used to collect the data (e.g., hardware apparatus or sensor, manual human curation, software program, software API)? How were these mechanisms or procedures validated?

A2: The data in FHA-Kitchens come from dataset publicly available datasets described above, which can be directly downloaded from their websites.

3. If the dataset is a sample from a larger set, what was the sampling strategy (e.g., deterministic, probabilistic with specific sampling probabilities)?

A3: Currently, we focus exclusively on hand interaction actions in kitchen scenes, thus primarily extracting data that includes hand interaction actions in kitchen scenes.

4. Who was involved in the data collection process (e.g., students, crowdworkers, contractors), and how were they compensated (e.g., how much were crowdworkers paid)?

A4: The authors and some volunteer undergraduate students from Wuhan University collected this dataset. The annotation compensation is based on the prevailing market rates.

5. Over what timeframe was the data collected? Does this timeframe match the creation timeframe of the data associated with the instances (e.g., the recent crawl of old news articles)? If not, please describe the timeframe in which the data associated with the instances was created.

A5: It took about 1 week to collect the data and about 6 weeks to complete organization and annotation (starting March 2023), as each participant labeled the bonding boxes and action triplets about four hours per workday. And the segmentation masks are generated by the Segment-Anything Model [75] guided by the bonding boxes, and corrected by human annotators for about one week.

A.3.4 Preprocessing/cleaning/labeling.

1. Was any preprocessing/cleaning/labeling of the data done (e.g., discretization or bucketing, tokenization, part-of-speech tagging, SIFT feature extraction, removal of instances, processing of missing values)? If so, please provide a description. If not, you may skip the remainder of the questions in this section.

A1: Yes. Since we focus on hand actions, we performed filtering and processing operations on the original videos, including the following three steps. (1) First, we observed that kitchen scenes often featured hand actions, with video content prominently showcasing human hand parts. Therefore, we sought out and extracted relevant videos that were set against a kitchen backdrop. (2) Then, to ensure the quality of the dataset, we selectively chose videos with higher resolutions. Specifically, 87% of the videos were recorded at 1,280 × 720 resolution, while another 13% had a shorter side of 480. Additionally, 67% of the videos were captured at 30 frames per second (fps), and another 33% were recorded at 24~25 fps. (3) Subsequently, we imposed a duration constraint on the videos, ranging from 30 seconds to 5 minutes, to exclude excessively long-duration videos. This constraint aimed to maintain a balanced distribution within the sample space. Finally, we collected a total of 2,377 video clips, amounting to 84.22 minutes of footage, encompassing 8 distinct types of dishes.

The collected video data was reorganized and cleaned to align with our annotation criteria. First, we split the collected video data into individual frames, as our annotated units are frames. Subsequently, we conducted further cleaning of the frames by excluding those that did not depict hands or exhibited meaningless hand actions. This cleaning process took into consideration factors such as occlusion, frame quality (i.e., without significant blur, subtitles, and logos), meaningful hand actions, and frame continuity. As a result, we obtained a total of 30,047 high-quality candidate video frames containing diverse hand actions for our FHA-Kitchens dataset. Compared to the initial collection, 113,436 frames were discarded during the cleaning process.

We recruited 10 voluntary annotators, whose responsibility was to annotate bounding boxes and multi-granularity action categories for each hand interaction region. To enhance annotation efficiency, we implemented a parallel annotation pipeline. The annotation of

fine-grained action triplets was carried out on the Amazon Mechanical Turk platform, while the bounding box and coarse-grained actions annotation was facilitated using the LabelBee tool. To ensure the annotation quality, three rounds of cross-checking and corrections were conducted.

2. Was the “raw” data saved in addition to the preprocessed/cleaned/ labeled data (e.g., to support unanticipated future uses)? If so, please provide a link or other access point to the “raw” data.

A2: No.

3. Is the software used to preprocess/clean/label the instances available? If so, please provide a link or other access point.

A3: The annotation of fine-grained action triplets was carried out on the Amazon Mechanical Turk platform, while the bounding box and coarse-grained actions annotation was facilitated using the LabelBee tool.

A.3.5 Uses.

1. Has the dataset been used for any tasks already? If so, please provide a description.

A1: No.

2. Is there a repository that links to any or all papers or systems that use the dataset? If so, please provide a link or other access point.

A2: N/A.

3. What (other) tasks could the dataset be used for?

A3: FHA-Kitchens can be used for the research of fine-grained hand action recognition, multi-granularity hand action detection, and interaction object detection. Besides, it can also be used for specific machine learning topics such as domain generalization and action segmentation. Please see Section 3.4 of the main paper and Section A.1.3 of the supplementary materials.

4. Is there anything about the composition of the dataset or the way it was collected and preprocessed/cleaned/labeled that might impact future uses? For example, is there anything that a future user might need to know to avoid uses that could result in unfair treatment of individuals or groups (e.g., stereotyping, quality of service issues) or other undesirable harms (e.g., financial harms, legal risks) If so, please provide a description. Is there anything a future user could do to mitigate these undesirable harms?

A4: No.

5. Are there tasks for which the dataset should not be used? If so, please provide a description.

A5: No.

A.3.6 Distribution.

1. Will the dataset be distributed to third parties outside of the entity (e.g., company, institution, organization) on behalf of which the dataset was created? If so, please provide a description.

A1: Yes. The dataset will be made publicly available to the research community.

2. How will the dataset will be distributed (e.g., tarball on website, API, GitHub)? Does the dataset have a digital object identifier (DOI)?

A2: It will be publicly available on the project website at GitHub

3. When will the dataset be distributed?

A3: We will distribute the dataset and related code soon.

4. Will the dataset be distributed under a copyright or other intellectual property (IP) license, and/or under applicable terms of use (ToU)? If so, please describe this license and/or ToU, and provide a link or other access point to, or otherwise reproduce, any relevant licensing terms or ToU, as well as any fees associated with these restrictions.

A4: It will be distributed under the MIT license.

5. Have any third parties imposed IP-based or other restrictions on the data associated with the instances? If so, please describe these restrictions, and provide a link or other access point to, or otherwise reproduce, any relevant licensing terms, as well as any fees associated with these restrictions.

A5: No.

6. Do any export controls or other regulatory restrictions apply to the dataset or to individual instances? If so, please describe these restrictions, and provide a link or other access point to, or otherwise reproduce, any supporting documentation.

A6: No.

A.3.7 Maintenance.

1. Who will be supporting/hosting/ maintaining the dataset?

A1: The authors.

2. How can the owner/curator/manager of the dataset be contacted (e.g., email address)?

A2: They can be contacted via email available on our dataset project website.

3. Is there an erratum? If so, please provide a link or other access point.

A3: No.

4. Will the dataset be updated (e.g., to correct labeling errors, add new instances, delete instances)? If so, please describe how often, by whom, and how updates will be communicated to users (e.g., mailing list, GitHub)?

A4: No. We have carefully three rounds of cross-checking the annotations to reduce the labeling errors. There may be very few labeling errors, which can be treated as noise.

5. Will older versions of the dataset continue to be supported/hosted/maintained? If so, please describe how. If not, please describe how its obsolescence will be communicated to users.

A5: N/A.

6. If others want to extend/augment/build on/contribute to the dataset, is there a mechanism for them to do so? If so, please provide a description. Will these contributions be validated/verified? If so, please describe how. If not, why not? Is there a process for communicating/distributing these contributions to other users? If so, please provide a description.

A6: N/A.

Table 15: Hyper-parameters used in MG-HAD.

Item	Value
lr	0.0001
lr_backbone	1e-05
weight_decay	0.0001
clip_max_norm	0.1
pe_temperature	20
enc_layers	6
dec_layers	6
dim_feedforward	2048
hidden_dim	256
dropout	0.0
nheads	8
num_queries	900
enc_n_points	4
dec_n_points	4
transformer_activation	“relu”
set_cost_class	2.0
set_cost_bbox	5.0
set_cost_giou	2.0
cls_loss_coef	1.0
bbox_loss_coef	5.0
giou_loss_coef	2.0
focal_alpha	0.25
dn_box_noise_scale (γ_1)	1.0
dn_label_noise_scale (γ_2)	0.5
subject_weight (w_s)	0.2
action_weight (w_a)	0.6
object_weight (w_o)	0.2

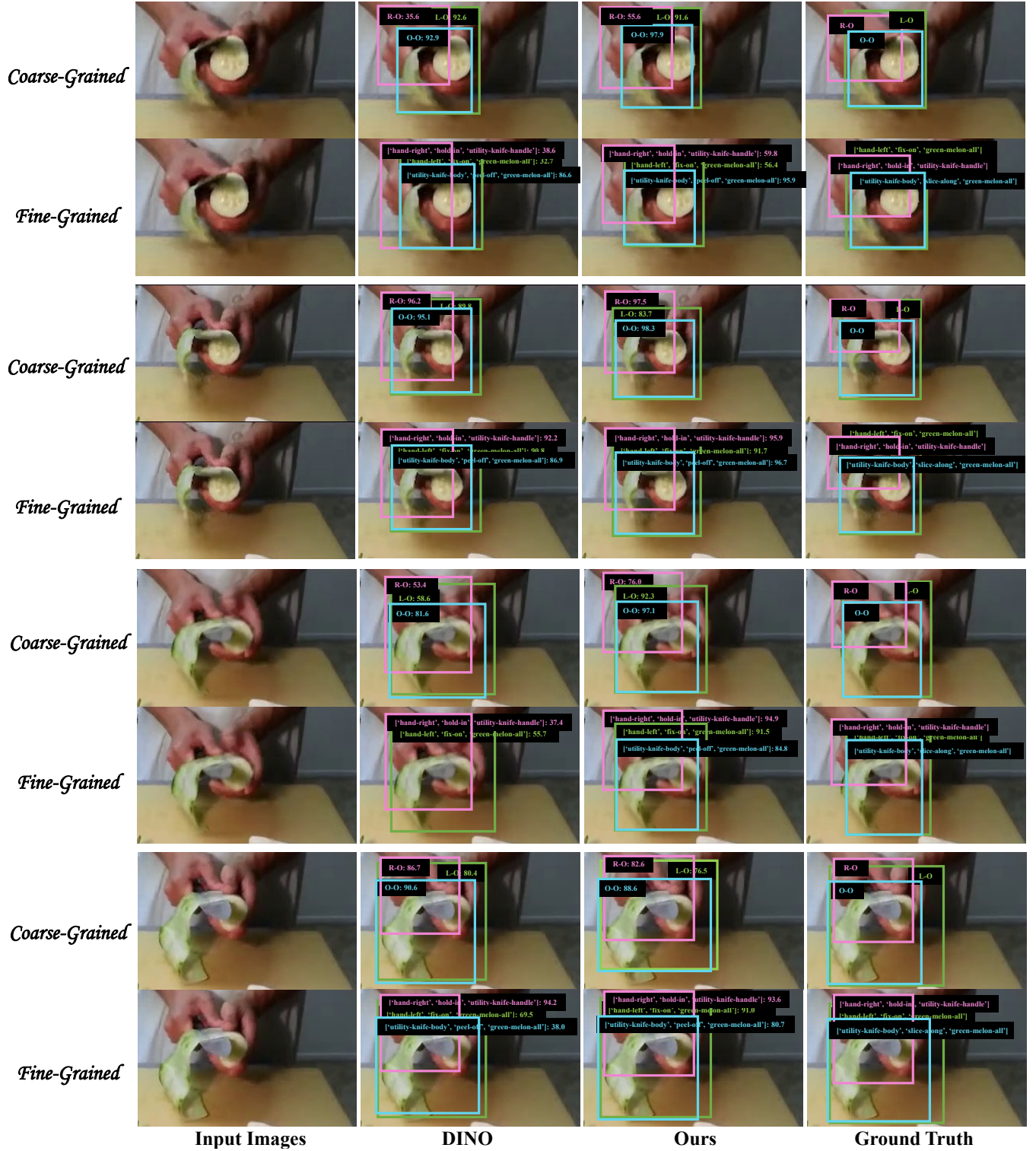


Figure 13: Qualitative comparison on the FHA-Kitchens dataset. Our model accurately detects three hand sub-interaction regions and provides multi-granularity hand action categories. Compared to the baseline [17], our model performs better across multi-dimensional fine-grained categories, demonstrating the effectiveness of our designed multi-dimensional action queries.

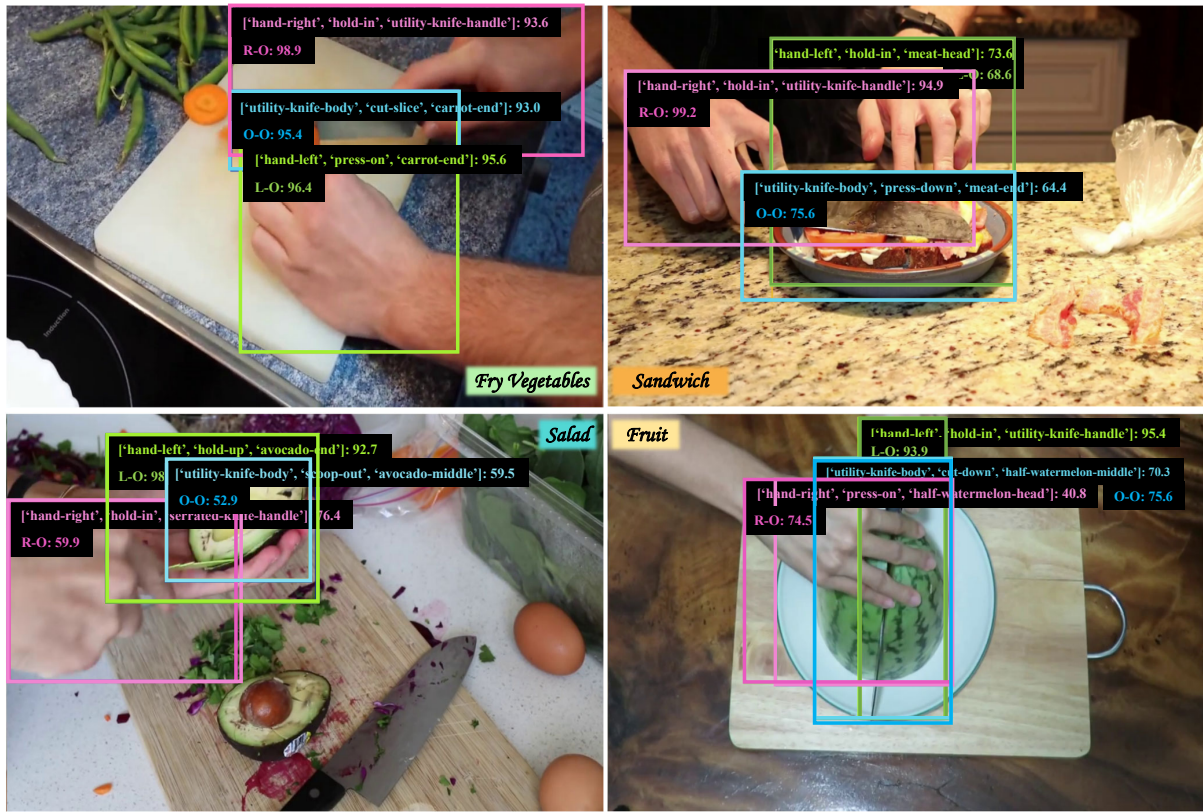


Figure 14: Visual detection results of our method in *four* different kitchens scenarios containing complex hand actions, *i.e.*, “*fry vegetables*”, “*sandwich*”, “*salad*”, and “*fruit*”. Our model offers accurate bounding boxes and multi-granularity hand action information for three hand sub-interaction regions.

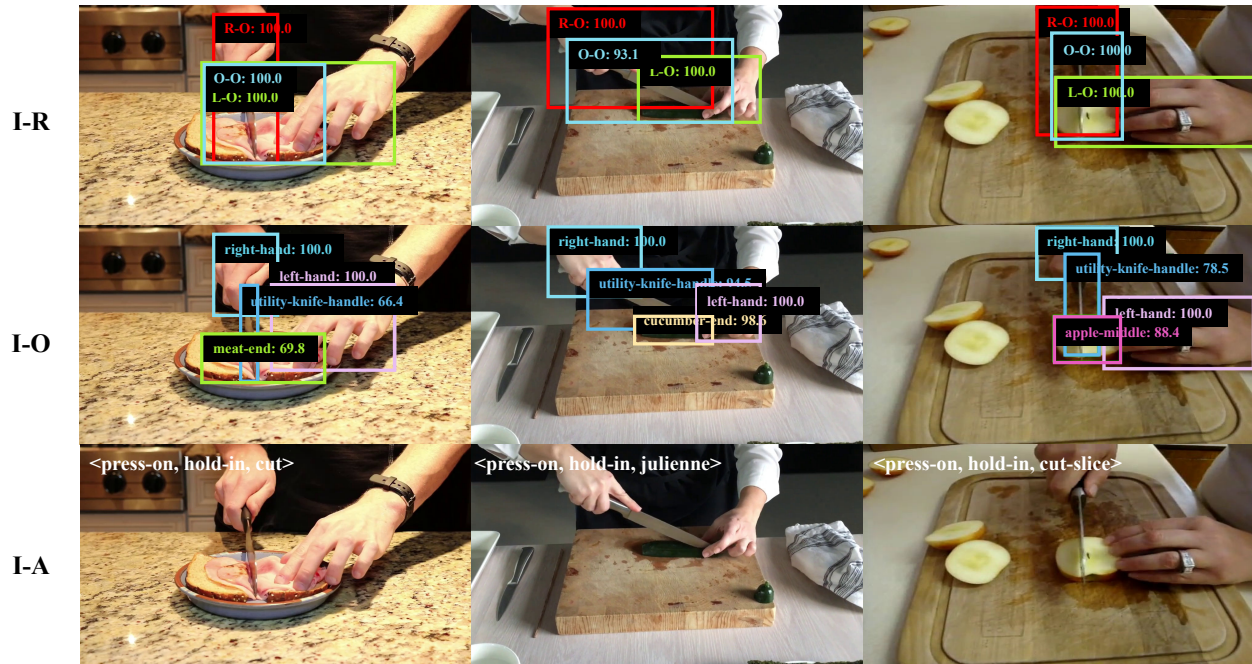


Figure 15: Visual results of Faster-RCNN [14] and TSN [11] methods in the SL-AD and SL-AR track experiments on our FHA-Kitchens dataset, showcasing interaction scenes with *three* hand sub-interaction regions, i.e., “Left hand-Object interaction region (L-O)”, “Right hand-Object interaction region (R-O)”, and “Object-Object interaction region (O-O)”. I-R: Interaction Region, I-O: Interaction Object, I-A: Interaction Region Action Verb.

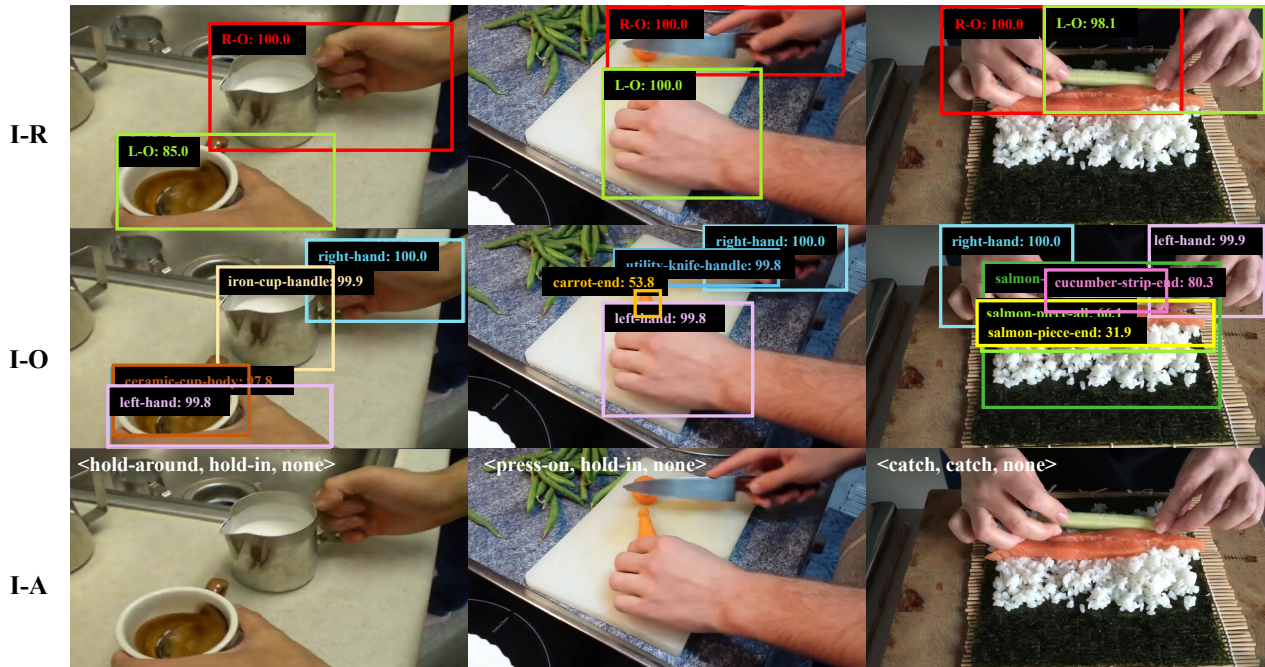


Figure 16: Visual results of Faster-RCNN [14] and TSN [11] methods in the SL-AD and SL-AR track experiments on our FHA-Kitchens dataset, showcasing interaction scenes with *two* hand sub-interaction regions, i.e., “Left hand-Object interaction region (L-O)” and “Right hand-Object interaction region (R-O)”. I-R: Interaction Region, I-O: Interaction Object, I-A: Interaction Region Action Verb.

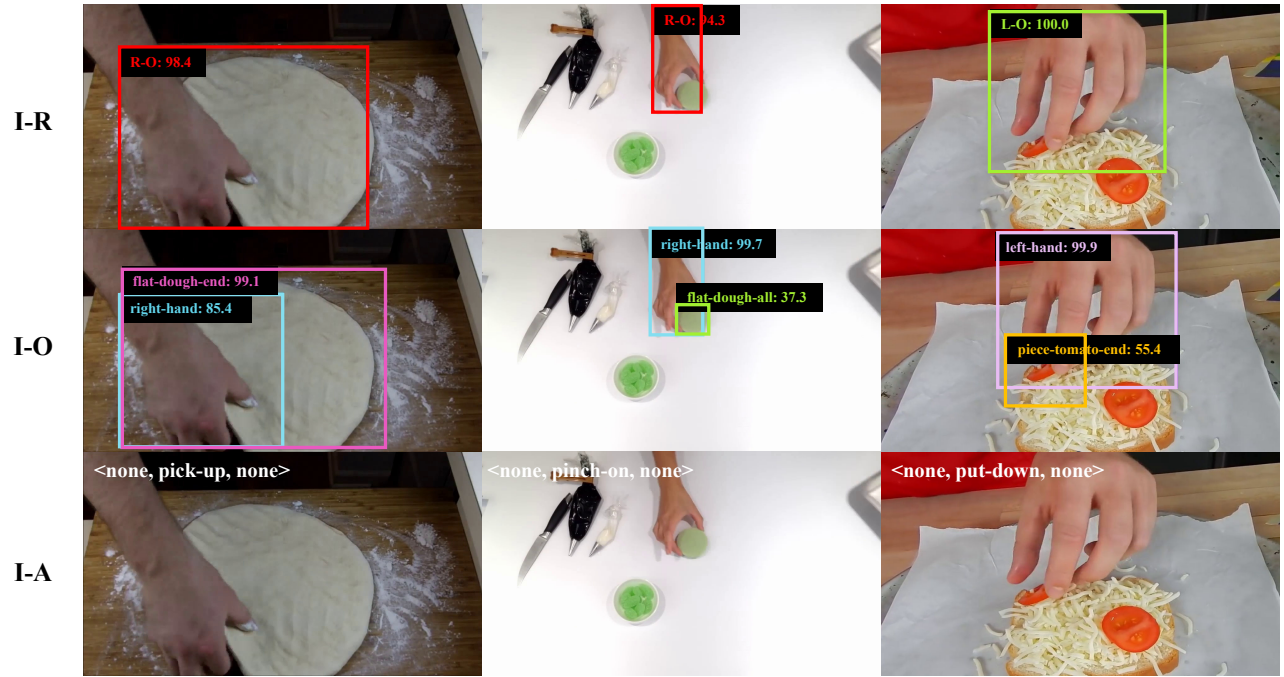


Figure 17: Visual results of Faster-RCNN [14] and TSN [11] methods in the SL-AD and SL-AR track experiments on our FHA-Kitchens dataset, showcasing interaction scenes with a *single* hand sub-interaction region, i.e., “Left hand-Object interaction region (L-O)” or “Right hand-Object interaction region (R-O)”. I-R: Interaction Region, I-O: Interaction Object, I-A: Interaction Region Action Verb.

Table 16: Vocabulary of fine-grained hand action verbs.

ID	Verb	#Instance	ID	Verb	#Instance
0	hold-around	1,593	65	knead	298
1	hold-at	788	66	contain	144
2	fill-with	265	67	roll-on	82
3	pinch-on	1,115	68	stick-to	50
4	rub-around	45	69	touch-to	12
5	hold-in	20,520	70	smooth-out	144
6	touch-on	42	71	sprinkle-on	203
7	hold-with	341	72	squeeze-around	189
8	press-on	9,369	73	press-down	675
9	cut-out	889	74	cut-up	100
10	fix-on	2,037	75	shovel-up	123
11	peel-off	1,413	76	grab-out	1
12	slice-along	1,306	77	close	51
13	grab	2,531	78	rotate	51
14	cut-half	230	79	open	72
15	take-up	134	80	open-down	27
16	pinch	609	81	hold-down	41
17	catch	446	82	cut-dice	443
18	put-down	1,406	83	dig-seeds	124
19	roll-up	1,296	84	chop	346
20	fix	293	85	push-forward	8
21	scrub-inside	53	86	cut-halves	22
22	lay-down	111	87	peel	87
23	hold-onto	453	88	push-ahead	2
24	pick-up	526	89	screw-on	5
25	cut-slice	2,808	90	sprinkle-into	16
26	take-out	178	91	scoop-up	85
27	turn-off	22	92	hold-along	129
28	cut-down	1,040	93	scrape-on	331
29	cut-off	820	94	stick-with	13
30	grab-up	115	95	cut-in	275
31	put-up	56	96	rub-on	11
32	break-apart	221	97	put-on	2
33	touch	483	98	push-off	10
34	cut-into-halves	136	99	place-on	17
35	bring-up	140	100	cut	15
36	pour-out	832	101	dip-in	9
37	pour-into	395	102	stretch-out	31
38	pour	154	103	flip	8
39	scrape	70	104	set-aside	22
40	rotate-around	162	105	julienne	165
41	screw-down	19	106	unroll	270
42	remove-out	69	107	adjust	46
43	hold-up	664	108	place-down	262
44	scoop-out	76	109	pile	49
45	open-up	21	110	pull	137
46	hold	946	111	attach-to	18
47	hold-on	187	112	grab-in	15
48	squeeze	334	113	knock-on	29
49	squeeze-out	254	114	press-against	13
50	mix-together	187	115	stir-in	114
51	spread-on	342	116	pull-up	47
52	twist-off	20	117	point-at	25
53	wrap-around	204	118	pull-out	33
54	break-off	417	119	scrape-down	6
55	grab-at	621	120	grab-onto	558
56	grab-on	384	121	hold-into	88
57	cut-through	25	122	hold-over	67
58	chop-dice	63	123	stir-into	49
58	chop-dice	63	124	press-onto	1
60	insert-into	106	125	roll	68
61	put-in	30	126	roll-out	33
62	dig-out	23	127	dip	51
63	cut-chunks	91	128	brush-onto	54
64	churn	369	129	flip-over	83

Table 17: Vocabulary of fine-grained interaction object nouns.

Super category	ID	Noun	#Instance	Super category	ID	Noun	#Instance
Vegetables&Plants	0	basil-end	201	Fruits	65	apple-all	22
	1	beet-end	143		66	apple-end	34
	2	beet-head	136		67	apple-head	253
	3	beet-middle	36		68	apple-middle	301
	4	bell-pepper-all	2		69	avocado-end	156
	5	bell-pepper-end	210		70	avocado-head	12
	6	bell-pepper-head	67		71	avocado-left	34
	7	bell-pepper-middle	139		72	avocado-middle	174
	8	broccoli-head	38		73	avocado-right	34
	9	carrot-end	1,625		74	block-watermelon-edge	5
	10	carrot-head	205		75	green-melon-all	4,074
	11	carrot-middle	638		76	green-melon-end	68
	12	chopped-vegetables-surface	38		77	green-melon-middle	68
	13	courgette-end	921		78	half-apple-head	139
	14	courgette-middle	39		79	half-apple-middle	47
	15	cucumber-end	288		80	half-pineapple-head	6
	16	cucumber-middle	165		81	half-pineapple-middle	99
	17	cucumber-strip-all	14		82	half-tomato-end	1
	18	cucumber-strip-end	72		83	half-tomato-middle	1
	19	cucumber-strip-middle	22		84	half-watermelon-edge	79
	20	garlic-middle	240		85	half-watermelon-end	17
	21	garlic-end	164		86	half-watermelon-head	301
	22	garlic-head	46		87	half-watermelon-middle	232
	23	ginger-end	248		88	lemon-end	156
	24	ginger-head	169		89	lemon-middle	108
	25	ginger-middle	70		90	melon-skin-all	119
	26	green-beans-end	937		91	melon-skin-end	576
	27	green-pepper-dice	1		92	melon-pulp-all	28
	28	green-pepper-end	710		93	melon-pulp-end	163
	29	green-pepper-head	142		94	melon-pulp-middle	49
	30	green-pepper-middle	505		95	melon-slice-end	200
	31	half-bell-pepper-end	116		96	orange-all	22
	32	half-bell-pepper-middle	110		97	orange-end	24
	33	half-onion-all	23		98	orange-head	209
	34	half-onion-head	11		99	orange-middle	547
	35	half-onion-middle	11		100	peelless-orange-middle	93
	36	mushroom-middle	15		101	piece-orange-edge	276
	37	nori-all	506		102	pineapple-all	26
	38	nori-end	262		103	pineapple-end	476
	39	onion-end	78		104	pineapple-head	959
	40	onion-head	28		105	pineapple-middle	1,346
	41	onion-middle	49		106	slice-pineapple-end	25
	42	pepper-seeds-all	4		107	slice-pineapple-middle	63
	43	piece-onion-middle	38		108	watermelon-edge	29
	44	piece-tomato-end	41		109	watermelon-end	966
	45	purple-cabbage-end	77		110	watermelon-head	155
	46	purple-cabbage-head	70		111	watermelon-middle	631
	47	purple-cabbage-middle	23	Dairy&Eggs	112	boiled-egg-end	226
	48	red-pepper-all	21		113	boiled-egg-head	22
	49	red-pepper-head	25		114	boiled-egg-middle	14
	50	red-pepper-middle	18		115	boiled-egg-shell	88
	51	small-tomato-head	9		116	egg-all	248
	52	small-tomato-middle	27		117	egg-head	1
	53	spinach-end	4		118	egg-middle	26
	54	spinach-head	35		119	egg-liquid-all	10
	55	spinach-middle	30		120	egg-shell-all	86
	56	spring-garlic-all	18		121	egg-shell-edge	34
	57	spring-garlic-end	53		122	milk-all	594
	58	spring-garlic-head	23		123	yolk-all	112
	59	spring-garlic-middle	52	Meat&Fish	124	chicken-dice	8
	60	sun-flower-seeds	104		125	raw-chicken-dice	69
	61	tomato-cube	22		126	crab-shred	328
	62	tomato-end	280		127	meat-end	515
	63	tomato-middle	17		128	meat-head	573
	64	tomato-sliced-middle	109		129	meat-middle	142

Table 18: Vocabulary of fine-grained interaction object nouns.

Super category	ID	Noun	#Instance	Super category	ID	Noun	#Instance
Meat&Fish	130	meat-piece-end	442	Containers	194	bottle-body	52
	131	meat-slice-all	1		195	box-lid-bottom	21
	132	meat-slice-end	202		196	bottle-cap	8
	133	piece-pepperoni-all	87		197	bottle-cap-all	106
	134	piece-pepperoni-end	158		198	bottle-cap-bottom	19
	135	salmon-piece-all	36		199	can-cover-edge	2
	136	salmon-piece-end	399		200	can-cover-edge	106
	137	salmon-piece-middle	14		201	ceramic-cup-all	68
	138	salmon-slice-end	44		202	ceramic-cup-body	671
Spices&Sauces	139	butter-all	45		203	ceramic-cup-handle	12
	140	crumbles-cheese-all	116		204	ceramic-lid-all	25
	141	cheese-all	27		205	ceramic-lid-edge	85
	142	green-butter-all	85		206	ceramic-teapot-handle	132
	143	mozzarella-all	84		207	ceramic-teacup-body	69
	144	mozzarella-end	12		208	ceramic-teacup-edge	138
	145	pizza-sauce-end	193		209	cup-edge	79
	146	powder-all	29		210	glass-bottle-edge	40
	147	sauce-all	397		211	glass-bottle-top	59
	148	slice-cheese-end	44		212	glass-cup-body	1
	149	tomato-sauce-all	151		213	glass-cup-edge	217
Liquids	150	tomato-sauce-edge	15		214	glass-cup-handle	51
	151	sauce-mixed	70		215	glass-goblet-stem	333
	152	can-opener	108		216	glastic-bottle-edge	4
	153	green-mixture-all	248		217	glastic-bottle-top	4
	154	jam-all	23		218	grass-bottle-top	30
Baked&Baking	155	oil-all	60		219	iron-basin-body	29
	156	olive-oil-all	51		220	iron-basin-edge	145
	157	baking-paper-edge	99		221	iron-basin-middle	115
	158	baking-paper-top	25		222	iron-cup-body	1,005
	159	baking-plate-edge	54		223	iron-cup-handle	325
Cooked Food	160	piece-pizza-end	125		224	iron-dipper-handle	14
	161	pizza-all	63		225	plastic-basin-edge	33
	162	pizza-end	27		226	plastic-bottle-bottom	21
	163	pizza-middle	29		227	plastic-bottle-edge	352
	164	sandwich-edge	32		228	plastic-bottle-top	78
	165	sandwich-end	297		229	plastic-cup-body	19
	166	sandwich-head	141		230	sauce-container-end	4
	167	sandwich-middle	123		231	small-cup-edge	195
	168	sandwich-side	85		232	small-plastic-bottle-edge	154
	169	sandwich-top	27		233	small-plastic-bottle-end	120
	170	sandwich-all	23		234	small-plastic-bottle-top	167
	171	sushi-roll-all	151		235	teapot-lid-edge	126
	172	sushi-roll-end	1,659		236	teapot-lid-handle	267
	173	sushi-roll-head	233		237	wine-bottle-bottom	75
	174	sushi-roll-middle	622		238	yogurt-box-bottom	63
Packaging	175	bamboo-mat-edge	284	Cutlery	239	yogurt-box-edge	62
	176	bamboo-mat-end	528		240	yogurt-box-handle	2
	177	bamboo-mat-head	8		241	yogurt-box-top	14
	178	bamboo-mat-middle	244		242	sauce-cup-all	9
	179	mozzarella-bag-end	71		243	bowl-bottom	69
	180	mozzarella-bag-middle	24		244	bowl-edge	198
	181	onion-bag-end	86		245	glass-bowl-all	23
	182	onion-bag-middle	30		246	glass-bowl-body	23
	183	pepperoni-bag-end	60		247	glass-bowl-bottom	91
	184	pepperoni-bag-middle	16		248	glass-bowl-edge	415
	185	pipng-bag-all	251		249	glass-bowl-handle	8
	186	pizza-box-edge	140		250	grass-bowl-edge	13
	187	tea-leaves-bag-body	38		251	green-bowl-edge	29
	188	tea-leaves-bag-bottom	42		252	small-bowl-edge	16
	189	tea-leaves-bag-top	38		253	steel-bowl-edge	153
Containers	190	black-bottle-top	42		254	steel-bowl-top	13
	191	bottle-all	1		255	metal-bowl-edge	470
	192	bottle-edge	19		256	plastic-bowl-all	46
	193	bottle-top	30				

Table 19: Vocabulary of fine-grained interaction object nouns.

Super category	ID	Noun	#Instance	Super category	ID	Noun	#Instance
Cutlery	257	plastic-bowl-body	10	Kitchenware	321	shovel-body	49
	258	plastic-bowl-edge	31		322	shovel-handle	49
	259	porcelain-bowl-edge	39		323	sieve-spoon-body	13
	260	porcelain-bowl-middle	2		324	sieve-spoon-handle	12
	261	porcelain-bowl-top	17		325	small-iron-pot-handle	90
	262	fork-handle	9		326	small-knife-body	663
	263	iron-spoon-body	353		327	small-knife-handle	706
	264	iron-spoon-handle	395		328	tea-strainer-body	108
	265	plastic-scoop-body	48		329	tea-strainer-edge	4
	266	plastic-scoop-handle	94		330	tea-strainer-handle	224
	267	plastic-spoon-body	22		331	turnplate-corner	15
	268	plastic-spoon-handle	22		332	turnplate-edge	9
	269	spoon-body	692		333	utility-knife-body	10,419
	270	spoon-handle	1,011		334	utility-knife-handle	11,157
	271	tablespoon-body	327		335	carrot-peeler-body	255
	272	tablespoon-handle	332		336	carrot-peeler-handle	518
	273	teaspoon-body	51	Appliances	337	grater-body	70
	274	teaspoon-handle	191		338	grater-handle	70
	275	wooden-spoon-body	116		339	oven-door-handle	22
	276	wooden-spoon-handle	152	Rice&Flour	340	ball-dough-end	27
	277	wooden-spatula-body	25		341	ball-dough-head	24
	278	wooden-spatula-handle	28		342	ball-dough-middle	173
	279	table-knife-handle	34		343	dough-all	413
	280	tableware-handle	11		344	dough-flour-all	117
Kitchenware	281	beater-end	25		345	dough-flour-middle	35
	282	plate-edge	335		346	flat-dough-all	42
	283	plate-end	20		347	flat-dough-edge	206
	284	brush-body	105		348	flat-dough-end	963
	285	brush-handle	195		349	flat-dough-middle	13
	286	can-opener-edge	83		350	flour-all	35
	287	can-opener-end	25		351	green-dough-all	123
	288	ceramic-plate-all	91		352	little-dough-al	1
	289	ceramic-plate-edge	208		353	little-dough-all	386
	290	chopping-board-edge	2		354	oval-dough-end	170
	291	cooking-spoon-body	77		355	rice-all	585
	292	cooking-spoon-handle	382		356	slice-bread-end	92
	293	food-mixer-handle	372		357	bread-end	510
	294	food-mixer	369		358	bread-head	199
	295	pizza-cutter-body	29		359	bread-middle	258
	296	pizza-cutter-handle	17	Dessert	360	chocolate-cake-edge	242
	297	food-plate-center	75		361	chocolate-cake-top	111
	298	food-plate-edge	36		362	chocolate-all	21
	299	handle	108		363	candies-all	159
	300	iron-plate-edge	76		364	candy-all	4
	301	kitchen-knife-body	552		365	candy-top	51
	302	kitchen-knife-handle	1,215		366	chocolate-bar-middle	87
	303	knife-body	26		367	chocolate-chips-all	49
	304	knife-handle	27		368	chocolate-cream-all	189
	305	jam-knife-body	50		369	chocolate-cream-top	261
	306	jam-knife-handle	53		370	chocolate-donut-all	35
	307	metal-plate-edge	47		371	cookie-all	41
	308	metal-spatula-body	71		372	cookie-end	57
	309	metal-spatula-handle	123		373	cookie-head	1
	310	pizza-spatula-body	70		374	cookies-all	49
	311	pizza-spatula-handle	99	Drink	375	cookie-top	9
	312	pizza-tray-edge	122		376	cream-all	139
	313	plastic-spatula-body	328		377	tea-all	14
	314	plastic-spatula-handle	531	Uncategorised	378	tea-leaves-all	219
	315	rolling-pin-body	198		379	whisk-head-top	9
	316	rolling-pin-handle	174		380	hand-left	23,305
	317	rolling-pin-middle	82		381	hand-right	26,441
	318	rolling-pin-middle	5		382	towel-all	82
	319	serrated-knife-body	38		383	towel-edge	38
	320	serrated-knife-handle	43				

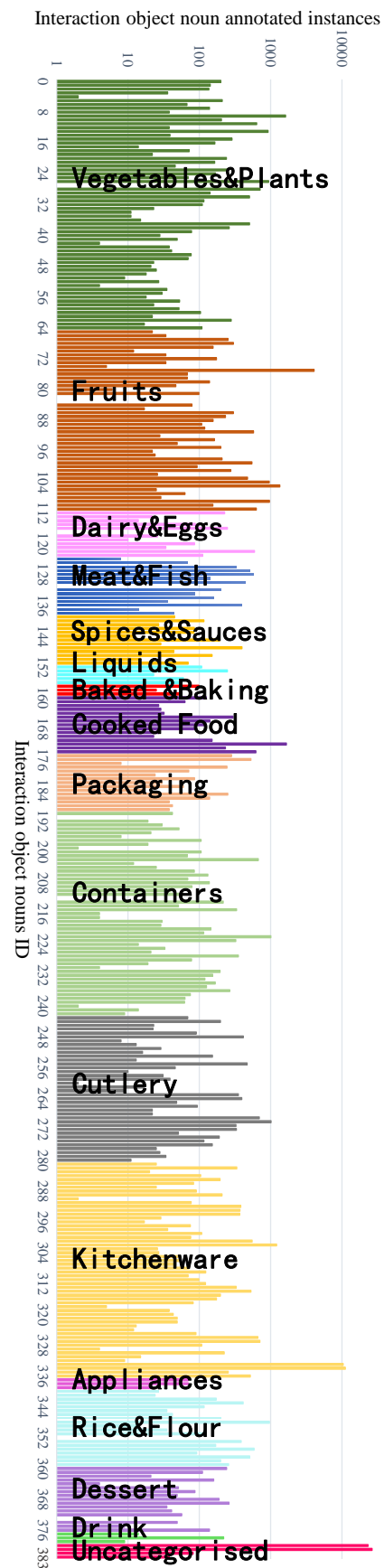


Figure 18: The distribution of instances per object noun category from 17 super-categories in the FHA-Kitchens dataset.